restricted by P-glycoprotein, a multi-drug efflux pump, and the tight junctions of brain capillary endothelial cells. CsA inhibited the function and expression of P-glycoprotein (Kochi *et al.*, 1999) and increased the permeability of brain endothelial cells (Dohgu *et al.*, 2000), suggesting that CsA could pass through the blood-brain barrier (BBB) due to the impaired function. In the present study, to test whether CsA induces neurotoxicity by passing through the damaged BBB and/or the reconstituted BBB with an incomplete function after an ischemic insult, we examined the effect of CsA on minimal electroshock-induced convulsions in mice treated with a transient middle cerebral artery occlusion (MCAO) for a short period (2 h).

MATERIALS AND METHODS

Male ddY mice weighing 25–35 g (Kyudo, Kumamoto, Japan) were housed in a room at a temperature of 22 ± 2°C under a 12-h light/dark schedule (lights on at 7:00 hours) and given water and food ad libitum. All the procedures involving experimental animals adhered to the law (No. 105) and notification (No. 6) of the Japanese Government, and were approved by the Laboratory Animal Care and Use Committee of Fukuoka University.

The pharmaceutical formulation of CsA (Sandimmun® injection, 250 mg/5 mL/ampule, Novartis Pharma, Tokyo, Japan) was used after a dilution with saline. The vehicle solution for CsA consisted of 13% polyoxyethylene castor oil (Cremophor EL®, Sigma, St. Louis, MO, USA), 7% ethanol, and 80% saline (the same mixture as the vehicle for Sandimmun® injection). A reagent for histological examination, 2,3,5-triphenyltetrazolium chloride (TTC), was purchased from Sigma.

Anesthesia was induced by 2% halothane (Flosen, Takeda, Osaka, Japan) and maintained with 1% halothane. Focal cerebral ischemia was induced by occlusion of the middle cerebral artery using the intraluminal filament technique (Mishima *et al.*, 2003). After a midline neck incision, the left common and external carotid arteries were isolated and ligated. An 8-0 nylon monofilament (Ethilon, Johinson & Johinson, Tokyo, Japan) coated with silicon resin (Xantopren, Heleus Dental Material, Osaka, Japan) was introduced through a small incision into the common carotid artery and was advanced to a position 9 mm distal from the carotid bifurcation for occlusion of the middle cerebral artery. Two hours after MCAO, animals were re-anesthetized with halothane, and reperfusion was established by withdrawal of the filament. The sham-operated mice were subjected to the procedure mentioned above without MCAO. At the end of the experiment, mice were decapitated under anesthesia with pentobarbital Na (40 mg/kg, i.p., Nembutal, Dainippon, Osaka, Japan) and brains were removed. Coronal sections were cut 2-mm thick and incubated in physiological saline containing 2% TTC at 37°C for 15 min for histological examination of the MCAO-induced brain damage.

Effect of CsA or vehicle on the minimal electroshock-induced convulsions was examined at 1, 3, 7 and 14 days after the sham-operation or MCAO. CsA (10 and 30 mg/kg) or vehicle was administered i.p. in a volume of 0.1 mL/10 g body weight. Sixty minutes after the injection, each mouse was subjected to the minimal electroshock (10 mA, at a frequency of 60 Hz, applied for 0.2 s) using

external corneal electrodes connected to an electroshock convulsive stimulator unit (MK-800, Muromachi Kikai, Tokyo, Japan) and placed individually in an acrylic cage (18 × 28 × 34 cm). The observations were made during a 2-min period with a camcorder (VL-DC1, Sharp, Tokyo, Japan) and stored on digital video tape. The durations of clonic and tonic-clonic convulsions were measured with a video player by two observers blinded to the pretreatment with CsA or vehicle. The minimal electroshock-induced convulsions were defined as positive when they lasted for more than 2 s. Only one of 12 normal mice showed convulsions for 1 s.

Statistical analysis was performed using Fisher's exact probability test. A value of $P < 0.05$ was considered significant.

RESULTS

Histological observations with TTC staining indicated that MCAO for 2 h produced a small infarcted region in the caudate putamen of the cerebral hemisphere with a relatively mild insult (an irregular pallor) at 1 day after the operation (Fig. 1). The size and intensity of infarction gradually increased in the cuadate putamen and cerebral cotex at 3–7 days, reaching a maximum at 14 days. Minimal electroshock did not induce convulsions in sham mice treated with vehicle. When CsA (10 or 30 mg/kg) was given, convulsions were induced by electroshock in 20–30% of sham mice at 1–14 days post-surgery (Fig. 2A). In MCAO mice treated with vehicle, electroshock-induced convulsion was observed in 1 of 8 mice at 1 day, but not at 3–14 days post-surgery (Fig. 2B). In MCAO mice, CsA (10 mg/kg) moderately increased the incidence of convulsions to 67% over the level in sham mice (20–30%) at 1 day but not at 3–14 days after operation (Fig. 2). CsA (30 mg/kg) markedly increased the incidence of convulsions to 90–100% at 1–7 days, but this increase was not observed at 14 days after the operation in MCAO mice (Fig. 2B).

DISCUSSION

Treatment with MCAO is employed to make an animal model of transient focal cerebral ischemia (Brown *et al.*, 1995; Sydserff *et al.*, 2002). In the present study, a short (2 h) MCAO produced small to mid-sized infarcted regions with increasing post-operative days in the caudate putamen and cerebral cortex, when compared with the usual MCAO method (4 h) (Mishima *et al.*, 2003) (Fig. 1).

A high dose of CsA (30 mg/kg) markedly aggravated the electroshock-induced convulsions in MCAO mice. This action appeared at an early stage (1–7 days) but not late stage (14 days) post-MCAO. An ischemic event has been known to cause disruption of the BBB (Cipolla *et al.*, 2004). Nishigaya *et al.* demonstrated using an immunohistological staining of endothelial barrier antigen that impairment and restoration of the brain endothelial barrier occurred in the post-ischemic period of 1–7 days and 14–28 days, respectively, in rats with MCAO for 2 h. Taken together with this evidence, the present findings suggest that CsA probably penetrates the brain through the impaired BBB at an early stage following ischemic insults and consequently has an adverse central action. The reconstituted BBB at a late-stage

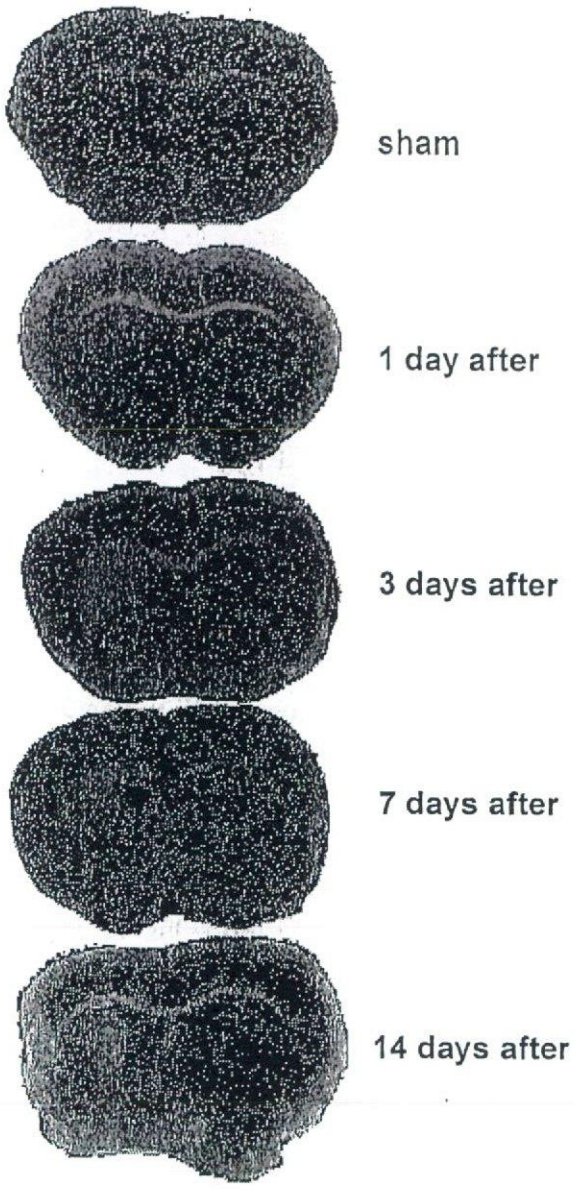

Fig. 1. Representative photographs showing coronal sections of the caudate putamen and cerebral cortex stained with 2% 2,3,5-triphenyltetrazolium chloride at 1, 3, 7 and 14 days after a transient middle cerebral artery occlusion for 2 h and at 7 days after sham operation (Sham).

post-MCAO may limit the delivery of CsA. Our previous findings *in vitro* demonstrated that CsA impairs brain endothelial barrier function by accelerating NO production in brain endothelial and astroglial cells (Ikesue *et al.*, 2000; Dohgu *et al.*, 2000; Yamauchi *et al.*, 2005). This action of CsA may be effective against the damaged BBB and/or the reconstituted BBB with an incomplete function at an early stage following the pathological insult. CsA is known to induce convulsions as a result of an

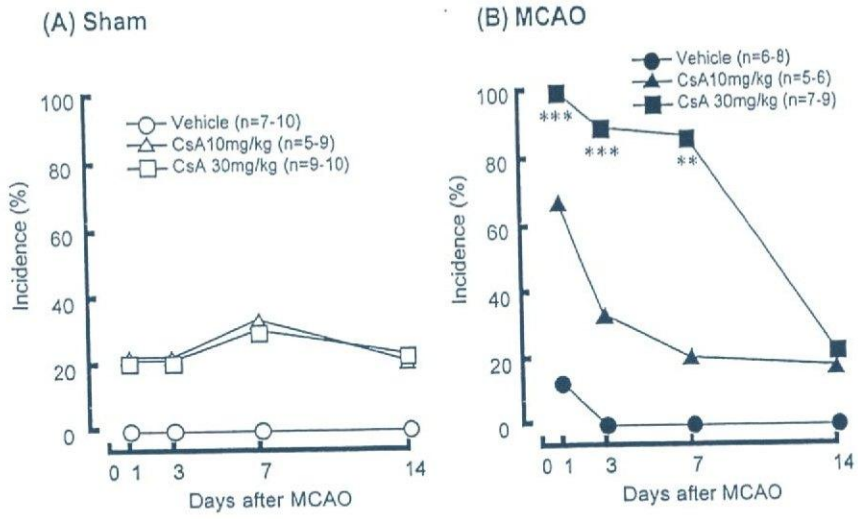

Fig. 2. Effect of cyclosporin A (CsA) on minimal electroshock-induced convulsions in sham-operated mice (Sham) (A) and in mice with a transient middle cerebral artery occlusion for 2 h (MCAO) (B). Values are expressed as the incidence (%) of convulsions in mice injected with vehicle or CsA 1 h before the test. The number of mice used in each treatment is indicated in parentheses. $^{**}P < 0.01$ and $^{***}P < 0.001$; significant difference from each corresponding group treated with vehicle.

interaction between NO and the γ-aminobutyric acid system in the hippocampus (Shuto *et al.*, 1999; Fujisaki *et al.*, 2002). This may be interpreted as a possible mechanism for the adverse central action of CsA after penetration of the brain. The possibility that MCAO influences these neuronal systems and increases the susceptibility to the deleterious effect of CsA on convulsions could not be excluded.

There is experimental evidence that CsA at low doses produces neuroprotective effects when given 30 min before or several minutes to 3 h after brain ischemia (Kuroda *et al.*, 1999; Yoshimoto *et al.*, 1999). In these studies, CsA prevented neuronal cell death including necrosis and apoptosis and decreased the infarct volumes in the brain. The different dosing schedule and doses of CsA are probably responsible for the discrepancy in the results.

In light of these findings, the possibility that CsA increases the risk of convulsions in patients with cerebral infarction and/or at an early stage following focal cerebral ischemia would have to be considered.

ACKNOWLEDGMENTS

This work was supported, in part, by Grants-in-Aid for Scientific Research ((B)(2) 14370789) and ((C)(2) 15590475) from JSPS, Japan, by a Grant-in-Aid for Exploratory Research (16659138) from MEXT, Japan, by funds (No.: 031001) from the Central Research Institute of Fukuoka University and by MEXT. HAITEKU (2000–2004).

0022-3565/05/3142-855–861$20.00
THE JOURNAL OF PHARMACOLOGY AND EXPERIMENTAL THERAPEUTICS
Copyright © 2005 by The American Society for Pharmacology and Experimental Therapeutics
JPET 314:855–861, 2005

Vol. 314, No. 2
85027/3042992
Printed in U.S.A.

Rapid Elimination of Cefaclor from the Cerebrospinal Fluid Is Mediated by a Benzylpenicillin-Sensitive Mechanism Distinct from Organic Anion Transporter 3

Misaki Kuroda, Hiroyuki Kusuhara, Hitoshi Endou, and Yuichi Sugiyama

Department of Molecular Pharmacokinetics, Graduate School of Pharmaceutical Sciences, University of Tokyo, Tokyo, Japan (M.K., H.K., Y.S.); and Department of Pharmacology and Toxicology, Kyorin University School of Medicine, Tokyo, Japan (H.E.)

Received February 15, 2005; accepted May 9, 2005

ABSTRACT

The purpose of this study was to investigate the carrier-mediated elimination of cephalosporins from the cerebrospinal fluid (CSF) via the choroid plexus. Cefaclor and cefalexin are structural analogs with similar lipophilicity, differing by only one functional group (cefaclor, –Cl; cephalexin, $-CH_3$), and they are substrates of rat peptide transporter PEPT2 with similar transport activities. However, cefaclor was cleared from the CSF more rapidly than cefalexin after intracerebroventricular administration (the elimination rate constants were 0.11 and 0.050 min^{-1}, respectively). The elimination of cefaclor from the CSF was inhibited by benzylpenicillin, but not by glycylsarcosine (GlySar), whereas GlySar, but not benzylpenicillin, had an inhibitory effect on the elimination of cefalexin from the CSF. The uptake of cefaclor by the freshly isolated rat choroid plexus was saturable, with a K_m value of 250 μM, and the uptake clearance corresponding to saturable components accounts for the major part of the in vivo clearance from the CSF (17 versus 26 μl/min, respectively). The uptake of cefaclor by the choroid plexus was inhibited by benzylpenicillin, but not by GlySar. However, the inhibitory effect of benzylpenicillin was weaker than expected from its own K_m value, and furthermore, organic anion transporter (Oat)3 substrates (cimetidine or *p*-aminohippurate) had no effect. These results suggest that cefaclor and cefalexin are eliminated from the CSF by different transporters, and rapid elimination of cefaclor from the CSF is accounted for by a benzylpenicillin-sensitive mechanism distinct from Oat3. A slight modification of a single chemical group of cephalosporins can greatly affect the contribution of the transporters involved, and their duration in the CSF.

The β-lactam antibiotics display a broad spectrum of antibacterial activity with a relatively low risk of allergic and toxic reactions, and cephalosporin antibiotics are prescribed widely throughout the world for the treatment of various infections, including bacterial meningitis (Dancer, 2001). Despite the availability of effective antimicrobial therapy, the morbidity and mortality associated with bacterial meningitis still remain significantly high, especially in developing countries (Tunkel and Scheld, 1997). As in other body sites, the bactericidal activity of cephalosporins in cerebrospinal fluid (CSF) predominantly depends on the length of time during which their concentrations exceed the minimum bactericidal concentrations of the infecting organisms. After intravenous administration, despite the similarity in their structures, various β-lactam antibiotics exhibit a noticeable difference in their distribution, which cannot be explained by their physicochemical properties.

Two major factors are known to determine the pharmacokinetics of β-lactam antibiotics in the CSF. One is their ability to cross the barriers of the central nervous system, which may be influenced by molecular size, their degree of plasma protein binding, and ionization (Levin, 1980; Spector, 1987). Another factor is their rate of efflux from the CSF via an active transport system in the choroid plexus, a leaf-like, highly vascularized organ that protrudes into the ventricles and is comprised of fenestrated capillaries surrounded by a tightly joined monolayer of epithelial cells (Spector, 1990; Suzuki et al., 1997). Quantitative studies of the distribution of β-lactam antibiotics in the CSF, using cefodizime (Nohjoh et al., 1989) and imipenem (Suzuki et al., 1989b) in comparison with benzylpenicillin, have also indicated that the CSF concentration of β-lactam antibiotics is greatly affected by their active elimination via the choroid plexus.

Recent progress in molecular cloning of transporter genes has identified the transporters involved in the elimination of

This work was supported by the research grant from the Ministry of Education, Culture, Sports, Science and Technology.
Article, publication date, and citation information can be found at http://jpet.aspetjournals.org.
doi:10.1124/jpet.105.085027.

ABBREVIATIONS: CSF, cerebrospinal fluid; OAT/Oat, organic anion transporter; PEPT, peptide transporter; GlySar, glycylsarcosine; HPLC, high-performance liquid chromatography.

drugs from the CSF, namely, organic anion transporters [Oat3/*Slc22a8* (Nagata et al., 2002) and Oatp1a5/*Slco1a5* (Kusuhara et al., 2003)] and a peptide transporter (PEPT2/*Slc15a2*) (Novotny et al., 2000). Both Oat3 and Oatp1a5 are characterized by their broad substrate specificity; Oat3 accepts amphipathic and hydrophilic organic anions as well as H_2 receptor antagonists as substrates (Kusuhara et al., 1999; Nagata et al., 2002, 2004a,b), whereas Oatp1a5 accepts amphipathic organic anions as substrates. Kinetic studies using Oat3 substrates and inhibitors suggest that Oat3 plays a major role in the uptake of hydrophilic organic anions such as benzylpenicillin, *p*-aminohippurate, and 2,4-dichlorophenoxyacetate (Nagata et al., 2002, 2004b) as well as cationic drugs; H_2 receptor antagonists (Nagata et al., 2004a) via the isolated rat choroid plexus; but not an amphipathic organic anion, estradiol 17β glucuronide, the uptake of which is mainly accounted for by Oatp1a5 (Kusuhara et al., 2003). PEPT2 has been reported to recognize various di- and tripeptides as well as peptide-mimetic drugs, including some β-lactam antibiotics, that contain an α-amino group in their structures, such as cefadroxil and cefalexin (Ganapathy et al., 1995; Daniel and Kottra, 2004; Smith et al., 2004). Using PEPT2 knockout mice, cefadroxil uptake by the freshly isolated choroid plexus has been shown to be mainly mediated by PEPT2 and partly by Oat3 (Ocheltree et al., 2004). Therefore, Oat3 and PEPT2 play important roles in regulating the CSF concentration of β-lactam antibiotics.

We found that after intracerebroventricular administration, cefalexin and cefaclor were eliminated from the CSF with different rate constants, even though they are structural analogs with similar lipophilicity (their apparent isobutylalcohol-buffer partition coefficients at pH 7.3 are 0.129 and 0.08 for cefaclor and cefalexin, respectively; Suzuki et al., 1987), differing by only one functional group (cefaclor, –Cl; cephalexin, $-CH_3$) (Fig. 1). The present study is aimed at characterizing the transport mechanisms accounting for the difference in the efflux rates of cefalexin and cefaclor. An inhibition study was carried out using benzylpenicillin and GlySar and showed that their inhibitory effect differed for the elimination of cefalexin and cefaclor, suggesting that different pathways were involved in the elimination of cefalexin and cefaclor from the CSF.

Materials and Methods

Materials. [^{14}C]Mannitol (56.0 mCi/mmol) was purchased from Amersham Biosciences UK, Ltd. (Little Chalfont, Buckinghamshire, UK), and [^{3}H]GlySar (4 Ci/mmol) was purchased from Moravek Biochemicals (Brea, CA). Unlabeled benzylpenicillin and cefalexin were purchased from Wako Pure Chemicals (Osaka, Japan), and other cephalosporins were obtained from Sigma-Aldrich (St. Louis, MO). All other chemicals and reagents were of analytical grade and were readily available from commercial sources. All cell culture media and reagents were purchased from Invitrogen (Carlsbad, CA), except for fetal bovine serum, which was obtained from Sigma-Aldrich.

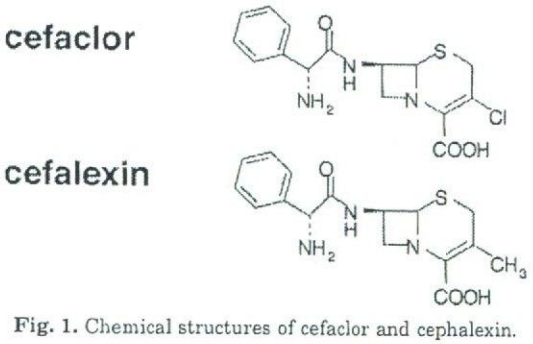

Fig. 1. Chemical structures of cefaclor and cephalexin.

Animals. Male Sprague-Dawley rats, weighing 220 to 240 g, were obtained from Japan SLC (Shizuoka, Japan), and experiments were carried out according to the guidelines provided by the Institutional Animal Care Committee (Graduate School of Pharmaceutical Sciences, University of Tokyo, Tokyo, Japan).

Construction of the LLC-PK1 Cell Line Stably Expressing Rat PEPT2 (PEPT2-LLC). Full-length PEPT2 cDNA was isolated from rat kidney mRNA and, after ligation into T vector (Promega, Madison, WI), was subcloned into pcDNA3.1 vector (Invitrogen) using NotI, SpeI, and XbaI. The construct was introduced into LLC-PK1 cells by LipofectAMINE (Invitrogen) according to the manufacturer's protocol, and stably transfected cells were selected by adding G418 sulfate (Invitrogen) to the culture medium. Five weeks after transfection, different clones were seeded on 12-well culture plates, and the transport activity was tested for positive clones.

Cell Culture. LLC-PK1 cells expressing rat Oat3 (Oat3-LLC) have been established previously (Sugiyama et al., 2001). Oat3- and newly established PEPT2-LLC were cultured on culture dishes in M199 (Invitrogen) supplemented with 10% fetal bovine serum, 100 U/ml penicillin, 100 μg/ml streptomycin, and 400 μg/ml G418 sulfate at 37°C with 5% CO_2 and 95% humidity. LLC-PK1 cells between passages 5 and 22 were used.

Transport Studies in cDNA-Transfected LLC-PK1 Cells. Cells were seeded in 12-well plates at a density of 1.2×10^5 cells/well for the transport studies. Twenty-four hours before beginning the assay, the cell culture medium was replaced with that containing 5 mM sodium butyrate to induce the expression of Oat3 and PEPT2.

Transport studies were carried out as described previously (Nagata et al., 2002). After cells were washed twice and preincubated with Krebs-Henseleit buffer at 37°C for 15 min, uptake was initiated by adding medium containing 1 μM unlabeled benzylpenicillin or GlySar in addition to 0.1 μCi of [^{3}H]benzylpenicillin or [^{3}H]GlySar. The Krebs-Henseleit buffer consisted of 118 mM NaCl, 23.8 mM $NaHCO_3$, 4.83 mM KCl, 0.96 mM KH_2PO_4, 1.20 mM $MgSO_4$, 12.5 mM HEPES, 5 mM glucose, and 1.53 mM $CaCl_2$, adjusted to pH 7.4. The uptake was terminated at designated time points by washing the cells twice with 1 ml of ice-cold Krebs-Henseleit buffer after removal of the incubation buffer. The cells were kept in 500 μl of 0.2 N NaOH overnight to allow lysis. After adding 100 μl of 1 N HCl, aliquots (400 μl) were transferred to scintillation vials containing 2 ml of scintillation fluid. The radioactivity associated with the cells and an aliquot of the incubation medium was determined using a liquid scintillation spectrophotometer (Amersham Biosciences, Inc., Piscataway, NJ) after the addition of scintillation fluid (Nacalai Tesque, Kyoto, Japan). Then, 50 μl of cell lysate was used to determine the protein concentration in each sample by the method of Lowry with bovine serum albumin as a standard.

Ligand uptake was given as the cell-to-medium concentration ratio determined as the amount of ligand accumulated in the cells divided by the medium concentration. Specific uptake was obtained by subtracting the uptake by vector-transfected cells from the uptake by cDNA-transfected cells. Inhibition studies were carried out by adding the desired concentrations of unlabeled inhibitors to the incubation medium.

Kinetic parameters were obtained using the following equation:

$$v = V_{max} \times S/(K_m + S) \quad (1)$$

where v is the uptake velocity of the substrate (picomoles per minute per milligram of protein), S is the substrate concentration in the medium (in micromolar), K_m is the Michaelis-Menten constant (in micromolar), and V_{max} is the maximum uptake rate (picomoles per minute per milligram of protein).

Inhibition constants (K_i values) of a series of compounds were obtained by examining their inhibitory effects on the Oat3- and PEPT2-mediated uptake. The substrate concentration was below the K_m values; thus, the inhibition constants can be obtained from the following equation, irrespective to the nature of the inhibition.

$$CL_{+I} = CL/(1 + I/K_i) \quad (2)$$

where CL is the uptake clearance, I is the concentration of inhibitor (in micromolar), and the subscript (+I) represents the value in the presence of inhibitor. Fitting was performed by the nonlinear least-squares method using a MULTI program (Yamaoka et al., 1981), and the Damping Gauss Newton Method algorithm was used for fitting.

Liquid Chromatography-Mass Spectrometry Analysis. The cellular accumulation of cefalexin and cefaclor by the cells and the medium concentration (45–55 μM) were quantified using liquid chromatography-mass spectrometry. Cefalexin and cefaclor in cell lysate were analyzed by liquid chromatography/mass spectrometry. The HPLC system consisted of a Separation Module (Waters 2695; Waters, Tokyo, Japan) connected to a Micromass ZQ with a ZSpray system (Waters). The system was controlled by version 3.5 of the Masslynx software. Chromatography was performed on a Capcell Pak C18 column (3 μm, 75 × 4.5 mm i.d.; Shiseido, Tokyo, Japan) protected by the same material. A gradient was applied using water (A) and acetonitrile (B), each containing 0.05% formic acid. The gradient conditions were as follows: initiate gradient with 100% A, ramp over 4 min to 30% A and 70% B, ramp over 1 min to 20% A and 80% B, hold for 0.5 min, and ramp over 0.1 min to 100% A to re-equilibrate the system. The total run time was 10 min. The compounds were eluted at a flow rate of 0.8 ml/min and allowed to pass into the electrospray source. The Micromass ZQ was operated in the atmospheric pressure chemical ionization-mass spectrometry positive ion mode with a corona current of 0.3 μA, cone voltage of 20 V, extractor voltage of 2.30 V, RF lens voltage of 0.3 V, source temperature of 100°C, cone temperature of 20°C, and desolvation temperature of 350°C. High-purity nitrogen gas was used as the desolvation gas at 300 ml/min, and the cone gas flow was 50 ml/min.

Intracerebroventricular Administration. The efflux of [^{3}H]GlySar after intracerebroventricular administration was studied using the method described previously in detail (Suzuki et al., 1989b; Ogawa et al., 1994). Rats were anesthetized with ketamine (60 mg/rat) and xylazine (0.984 mg/rat), and their heads were fixed in a stereotaxic apparatus. A hole was drilled in the skull, 1.5 mm to the left and 0.5 mm posterior to the bregma, into which a needle was fixed as a cannula for injection. An intracerebroventricular dose of [^{3}H]GlySar (20 nCi/rat) and [^{14}C]mannitol (0.4 nCi/rat), dissolved in 10 μl of artificial CSF, was administered to the left lateral ventricle. The prepared artificial CSF consisted of 122 mM NaCl, 25 mM $NaHCO_3$, 10 mM glucose, 3 mM KCl, 1.4 mM $CaCl_2$, 1.2 mM $MgSO_4$, 0.4 mM K_2HPO_4, and 10 mM HEPES, adjusted to pH 7.3. For inhibition studies, unlabeled inhibitors of desired concentrations were administered simultaneously. At designated times, 50 to 100 μl of CSF was withdrawn by cisternal puncture and centrifuged to remove any contaminating blood. The remaining radioactivity in the CSF specimens was determined using a liquid scintillation spectrophotometer after the addition of scintillation fluid, and the elimination rate was calculated. Intracerebroventricular administration of cefaclor or cefalexin (1.25 μg/rat) and [^{14}C]mannitol (0.4 nCi/rat) was performed using the same method. The CSF specimens were subjected to HPLC analysis for quantification of cefalexin and cefaclor; and for [^{3}H]mannitol, the radioactivities associated with the CSF specimens were determined in a liquid scintillation spectrophotometer after addition of scintillation fluid. The elimination clearance from the CSF was determined by multiplying the elimination rate constant by the volume of CSF. In the present study, 250 μl was used as the volume of CSF (Cserr and Berman, 1978).

Transport Studies Using Isolated Rat Choroid Plexus. The uptake of [^{3}H]GlySar by rat choroid plexus was examined using the method described previously (Nagata et al., 2002). The choroid plexus was isolated from the lateral ventricles of SD rats and incubated at 37°C for 1 min in 500 μl of artificial CSF, consisting of 122 mM NaCl, 25 mM $NaHCO_3$, 10 mM glucose, 3 mM KCl, 1.4 mM $CaCl_2$, 1.2 mM $MgSO_4$, 0.4 mM K_2HPO_4, and 10 mM HEPES, equilibrated with 95% O_2/5% CO_2, and adjusted to pH 7.4. Incubation medium containing ligands, with or without inhibitors, was added to initiate uptake and at designated time points, the choroid plexus was washed three times in ice-cold artificial CSF to terminate the uptake. The tissue-to-medium concentration ratios of ligands were calculated with [^{14}C]urea as a cell water space marker. The ^{3}H and ^{14}C activity of the specimens was determined in a liquid scintillation spectrophotometer. The uptake of cefaclor by rat choroid plexus was examined as described above, and the samples were analyzed by HPLC. The uptake of cefaclor by the isolated rat choroid plexus was determined at different substrate concentrations ranging from 10 μM to 10 mM, and the effects of benzylpenicillin, GlySar, cimetidine, and *p*-aminohippurate were investigated at designated concentrations.

HPLC Assay. Concentrations of cefalexin and cefaclor in CSF and in the choroid plexus were analyzed by HPLC. The HPLC system included a pump (L-6200 intelligent pump; Hitachi, Ibaraki, Japan), a YMC-Pack Pro C18 column (5 μm, 250 × 4.6 mm; YMC, Tokyo, Japan) protected by the same material, a column oven (L-7300; Hitachi) set at 40°C, and a UV detector (L-4200 UV-VIS detector; Hitachi) operated at 260 nm. The system was controlled by an L-7200 autosampler (Hitachi). The mobile phase consisted of 0.01 M acetic acid, pH 4.7/methanol/2-propanol (80:20:1). The compounds were eluted at a flow rate of 1.0 ml/min.

Statistical Analysis. Statistical analysis of the effect of inhibitors on the uptake of cefaclor by the freshly isolated rat choroid plexus was performed by one-way analysis of variance followed by Fisher's t test to identify significant differences.

Results

Uptake of GlySar, Cefalexin, and Cefaclor by PEPT2-LLC. Transfection of rat PEPT2 cDNA increased the uptake of GlySar, a typical substrate of PEPT2 (Fig. 2A). The concentration dependence of the uptake of GlySar by PEPT2 was determined after a 3-min incubation. Nonlinear regression analysis yielded K_m and V_{max} values of 172 ± 21 μM and 2340 ± 240 pmol/min/mg protein, respectively (Fig. 2B).

Figure 2C shows the time profiles of the uptake of cefaclor and cefalexin by PEPT2. As for GlySar, the uptake of cefaclor and cefalexin was significantly greater in PEPT2-LLC than in vector-LLC. The K_i values of cefaclor for GlySar uptake by PEPT2 were determined to be 171 ± 27 μM (Fig. 2D).

Effect of Cefaclor, Cefadroxil, and Cefalexin on Benzylpenicillin Uptake by Oat3-LLC. The uptake of benzylpenicillin by Oat3- and vector-LLC for 5 min was 27.5 ± 2.1 and 5.32 ± 0.30 μl/mg protein, respectively. The uptake of cefaclor was determined in Oat3- and vector-LLC. It was found that they were comparable, and no specific uptake of cefaclor was detected by Oat3 (data not shown). The inhibitory effect of cefaclor, cephalexin, and cefadroxil on the uptake of benzylpenicillin by Oat3-LLC for 5 min was examined (Fig. 3). Cefaclor showed moderate potency, whereas cefalexin and cefadroxil showed weak potency. The K_i values of cefaclor, cephalexin, and cefadroxil were determined to be 105 ± 24, 677 ± 143, and 1060 ± 210 μM, respectively.

Elimination of GlySar, Cefalexin, and Cefaclor from CSF after Intracerebroventricular Administration. Figure 4 shows the CSF concentration of GlySar, cephalexin, or cefaclor and mannitol after intracerebroventricular ad-

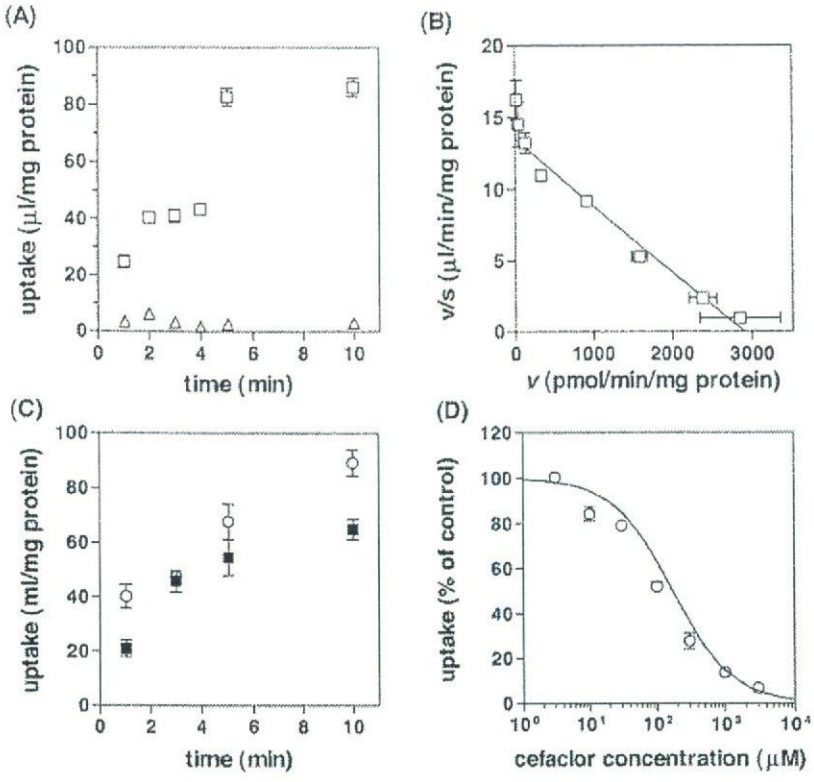

Fig. 2. Time-profile of the uptake of GlySar, cefalexin, and cefaclor by PEPT2-LLC, and the effect of cefaclor on PEPT2-mediated GlySar uptake. A, uptake of 1 μM GlySar by PEPT2-LLC (squares) and also by vector-LLC (triangles) was determined. B, concentration dependence of the uptake of GlySar by PEPT2 was determined after a 3-min incubation. The uptake was determined at different substrate concentrations (1 μM–3 mM). The fitted line was converted to the v/s versus v form (Eadie-Hofstee plot). C, uptake of 50 μM cefalexin (closed squares) and 54 μM cefaclor (open circles) by PEPT2-LLC was determined, and their uptake by vector-LLC was below the detection limit. D, uptake of [^{3}H]GlySar by PEPT2-LLC was determined after a 3-min incubation in the presence and absence of cefaclor at designated concentrations. Each point represents the mean ± S.E. (n = 3).

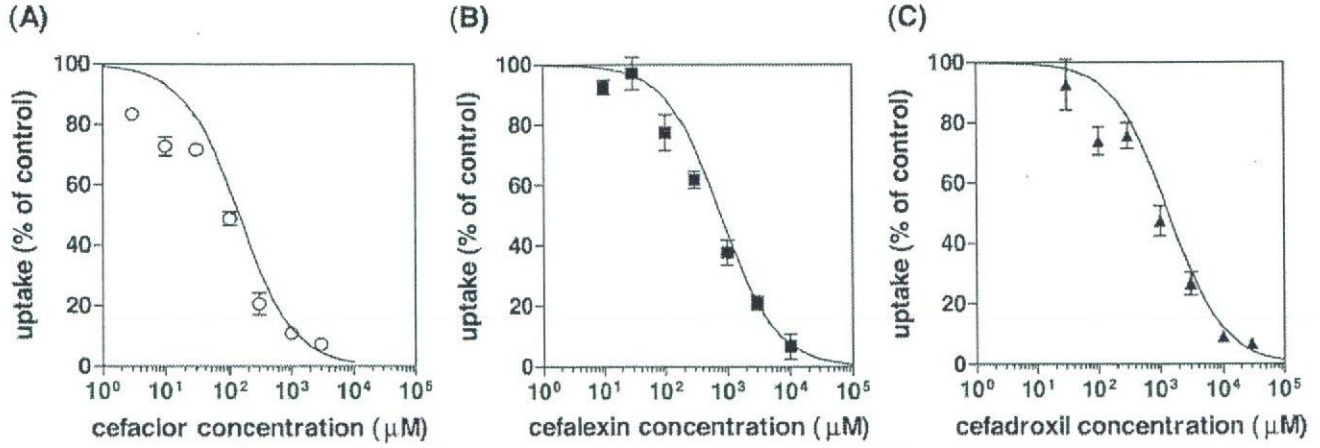

Fig. 3. Effect of cephalosporins on the uptake of [^{3}H]benzylpenicillin by Oat3-LLC. The uptake of [^{3}H]benzylpenicillin by Oat3-LLC was determined after a 5-min incubation in the presence and absence of the cephalosporins cefaclor (A), cefalexin (B), and cefadroxil (C) at the designated concentrations. Each point represents the mean ± S.E. (n = 3). The solid line represents the fitted line. Details of fitting are described under *Materials and Methods*.

ministration as a function of time. GlySar was eliminated from the CSF with a greater rate constant than mannitol, a reference compound for CSF turnover and diffusion into the brain interstitial space through the ependyma surface, with a rate constant of 0.073 min^{-1}. The elimination clearance of GlySar from the CSF (18 μl/min) was 2.5-fold greater than that of mannitol (7.23 ± 2.49 μl/min). The elimination of GlySar was saturated at the concentration examined (3 mM), whereas simultaneous injection of benzylpenicillin had no effect at a concentration sufficiently high to saturate its own elimination (Ogawa et al., 1994) (Fig. 5A).

Cefalexin was eliminated from the CSF with a rate constant of 0.0504 ± 0.0228 min^{-1} after intracerebroventricular administration (Fig. 4B), whereas cefaclor was more rapidly eliminated from the CSF with an elimination rate constant of 0.105 ± 0.002 min^{-1} (Fig. 4C). The elimination clearances of cefalexin and cefaclor were 13.0 ± 5.7 and 26.3 ± 0.5 μl/min, respectively. The elimination of both cephalosporins from the CSF was saturable, suggesting the involvement of a transporter (Fig. 5). Furthermore, the elimination of cefalexin was inhibited by GlySar, but it was not significantly affected by benzylpenicillin (Fig. 5B). Conversely, the elimination of cefaclor was inhibited by benzylpenicillin, but not by GlySar (Fig. 5C).

Uptake of Cefaclor by Isolated Rat Choroid Plexus. The uptake of cefaclor by freshly isolated rat choroid plexus was determined (Fig. 6A). The accumulation of cefaclor in the choroid plexus increased linearly for up to 5 min of incuba-

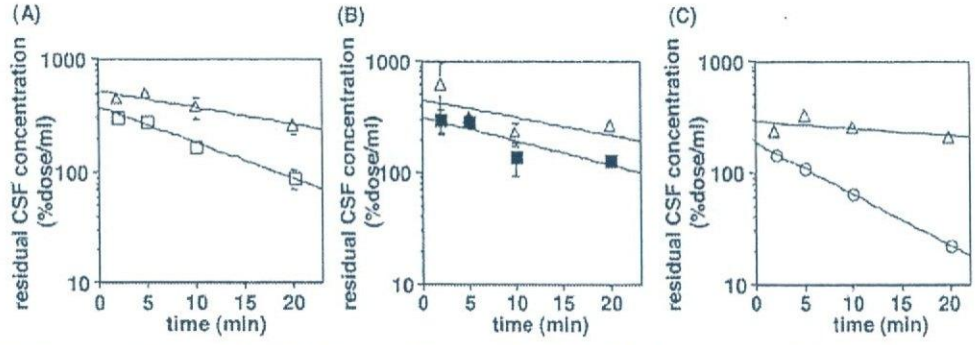

Fig. 4. CSF concentration versus time profiles of GlySar, cephalexin, and cefaclor after intracerebroventricular administration. [^{3}H]GlySar (A), cefalexin (B), and cefaclor (C) were administered into the lateral ventricle of rats. The initial concentration of [^{3}H]GlySar was 20 nM in the CSF, whereas that of cefalexin and cefaclor was 13 μM. The concentration of ligand remaining in the cisternal CSF was determined at the designated times. [^{14}C]Mannitol (open triangles) was coadministered as a reference for CSF turnover and passive diffusion into the brain parenchyma. The values are expressed as the percentage of the dose remaining per milliliter of CSF. Each point represents the mean ± S.E. of triplicate determinations using three rats. The solid lines represent the fitted elimination curve.

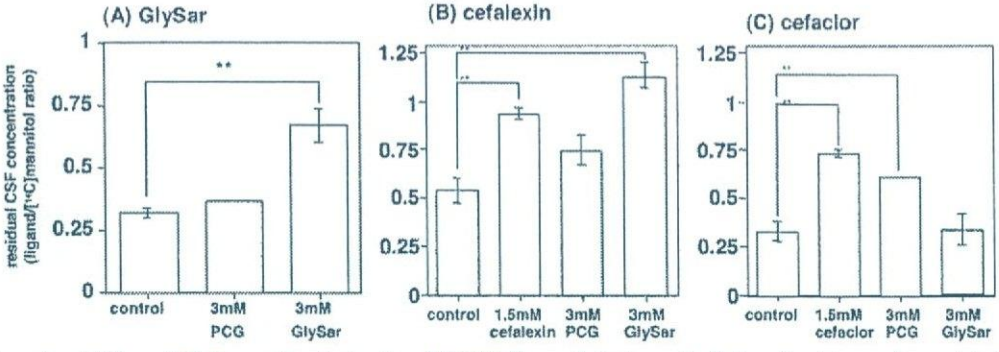

Fig. 5. Effects of benzylpenicillin and GlySar on the elimination of [^{3}H]GlySar, cephalexin, and cefaclor after intracerebroventricular administration. [^{3}H]GlySar (A), cefalexin (B), and cefaclor (C) were administered into the lateral ventricles of rats in the presence or absence of unlabeled benzylpenicillin (PCG) or GlySar. The designated concentrations represent their concentration in the CSF after injection. The concentration of ligand remaining in the cisternal CSF was determined at 20 min. [^{14}C]Mannitol was coadministered as a reference. The values are expressed as a ratio of the percentage of remaining ligand and [^{14}C]mannitol. Each point represents the mean ± S.E. of triplicate determinants using three rats. **, $p < 0.01$ (Student's t test).

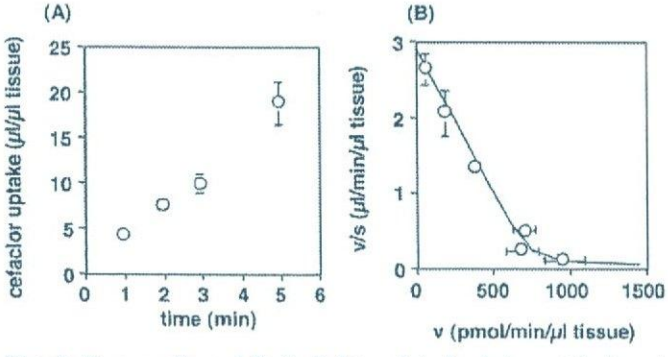

Fig. 6. Time profile and Eadie-Hofstee plot of cefaclor uptake by rat isolated choroid plexus. The uptake of 20 μM cefaclor was examined in the presence or absence of unlabeled cefaclor. The concentration dependence was determined after a 5-min incubation. The solid line represents the fitted line that was converted to the v/s versus v form (Eadie-Hofstee plot). The details of the fitting are described under *Materials and Methods*. Each point represents the mean ± S.E. of quadruple determinations.

tion; therefore, further studies were carried out at 5 min. Kinetic analyses based on Akaike's information criteria revealed that the K_m and V_{max} values for cefaclor uptake by rat isolated choroid plexus were 251 ± 31 μM and 722 ± 62 pmol/min/μl tissue, respectively, and the clearance corresponding to the nonsaturable component was 0.0242 ± 0.0099 μl/min/μl tissue (Fig. 6B). Inhibition studies were carried out to characterize the uptake of cefaclor by freshly isolated rat choroid plexus. Benzylpenicillin exhibited a significant inhibitory effect on the uptake in a concentration-dependent manner, and 3 mM benzylpenicillin had a significant effect (Fig. 7). In contrast, GlySar, cimetidine or p-aminohippurate had no significant inhibitory effect (Fig. 7).

Discussion

The efflux mechanisms in the choroid plexus have been shown to be an important factor governing the CSF concentration of β-lactam antibiotics and their therapeutic efficacy in bacterial meningitis. Regarding the efflux transport of β-lactam antibiotics from the CSF, Oat3 has been suggested to be responsible for the elimination of benzylpenicillin from the CSF and partly of the cephalosporin cefadroxil (Nagata et al., 2002; Ocheltree et al., 2004), whereas PEPT2 has been suggested to play a role in the elimination of cephalosporins with an α-amino group (Smith et al., 2004). In the present study, the elimination profiles of the analogs cefalexin and cefaclor from the CSF were compared after intracerebroventricular administration, and the uptake of cefaclor by the freshly isolated rat choroid plexus was characterized. Transport studies using the PEPT2-cDNA transfectant showed that both cefaclor and cefalexin are substrates of PEPT2 with

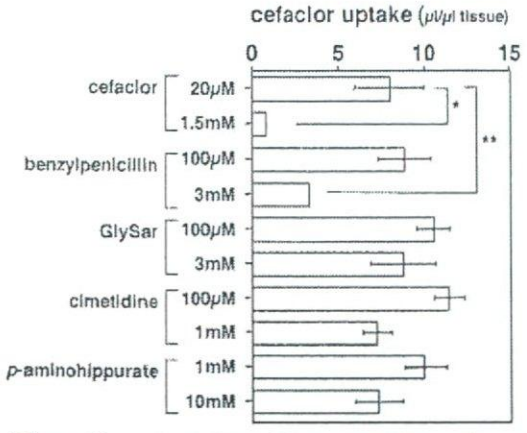

Fig. 7. Effects of benzylpenicillin, GlySar, cimetidine, and *p*-aminohippurate on the uptake of cefaclor by freshly isolated rat choroid plexus. The uptake of 20 μM cefaclor was determined at 5 min in the presence or absence of inhibitors at designated concentration. Each point represents the mean ± S.E. of quadruple determinations. **, $p < 0.01$; *, $p < 0.05$.

similar transport activities (Fig. 2). For Oat3, although the cephalosporins had a moderate or weak inhibitory effect (Fig. 3), no specific uptake of cefaclor by Oat3 could be detected (data not shown).

After intracerebroventricular administration, the elimination rates of cefalexin and cefaclor from the CSF were different. The elimination clearance of cefaclor from the CSF was 2-fold greater than that of cefalexin. Taking into consideration the clearance by nonspecific elimination pathways, such as a convective flow associated with CSF turnover and diffusion into the brain parenchyma across the ependyma surface, there was a 3-fold difference in the efflux clearance across the choroid plexus between cefaclor and cefalexin. To characterize the efflux transport, an in vivo inhibition study was carried out using benzylpenicillin and GlySar as inhibitors. It was found that there was a clear difference in the inhibition potencies of these inhibitors for the elimination of cefalexin and cefaclor from the CSF (Fig. 5), suggesting a difference in the contribution of the transporters responsible, despite their analogous chemical structures.

Furthermore, the uptake of cefaclor by isolated rat choroid plexus was characterized. Time-dependent and saturable uptake of cefaclor was observed in the freshly isolated rat choroid plexus (Fig. 6). Taking the water space of the rat choroid plexus (6 μl/rat) into consideration (Ogawa et al., 1994), it would be expected that the uptake clearance corresponding to the saturable fraction would account for the major part of the elimination clearance from the CSF (17 versus 26 μl/min/rat, respectively). Consistent with the in vivo observation (Fig. 5), benzylpenicillin had a significant effect on the uptake of cefaclor by the freshly isolated rat choroid plexus, whereas GlySar had no significant effect (Fig. 7). The uptake of benzylpenicillin by the isolated rat choroid plexus has been shown to be carrier-mediated (Suzuki et al., 1987; Nagata et al., 2002). However, its inhibition of the uptake of cefaclor was lower than expected from its own K_m value [58 μM (Suzuki et al., 1987), 111 μM (Nagata et al., 2002)] (Fig. 7). Furthermore, *p*-aminohippurate and cimetidine had no effect (Fig. 7), even at a concentration sufficient to inhibit benzylpenicillin uptake in the choroid plexus (Nagata et al., 2002). These kinetic results suggest that benzylpenicillin and cefaclor do not share the same uptake mechanism at the choroid plexus.

Considering the previous result obtained using another analog, cefadroxil (Ocheltree et al., 2004), PEPT2 is one of the candidate transporters responsible for the uptake of cefalexin by the choroid plexus. Inhibition of its elimination from the CSF by GlySar supports this hypothesis. In contrast to these analogs, the absence of inhibitory effect of GlySar on the elimination of cefaclor suggests a minimal contribution from PEPT2. Instead, a benzylpenicillin-sensitive transporter, distinct from the classical transporter responsible for benzylpenicillin uptake in the choroid plexus, accounts for the uptake of cefaclor by the choroid plexus and the rapid elimination of cefaclor from the CSF.

The present study demonstrates that even a minor modification of a single chemical group can dramatically alter the CSF retention time. Changing the methyl group of cefalexin to chloride alters the contribution of the responsible transporters, resulting in a marked increase in the elimination clearance across the choroid plexus. As discussed by Ocheltree et al. (2004), several cephalosporins without an α-amino group can achieve clinically adequate CSF concentrations for the treatment of bacterial meningitis. These clinical observations suggest that the α-amino group is also required for substrate recognition by the benzylpenicillin-sensitive transporter. This should be investigated further in future studies to establish a rational strategy for chemical modification to regulate the CSF concentrations of cephalosporins.

In addition to the CSF, it has been found that the brain parenchyma is the target of β-lactam antibiotics to prevent glutamate neurotoxicity through induction of glutamate transporters (Rothstein et al., 2005). The delivery of β-lactam antibiotics to the brain will become more important in future as far as increasing their therapeutic efficacy is concerned. There is another barrier, the blood-brain barrier, formed by a tight monolayer of brain capillary endothelial cells, in the central nervous system that prevents the passage of drugs into the central nervous system from the circulating blood. It has been suggested that the uptake of benzylpenicillin and cefodizime by the brain from the blood is mediated by a transporter (Suzuki et al., 1989a; Matsushita et al., 1991). However, benzylpenicillin has been suggested to undergo efflux across the blood-brain barrier, presumably by Oat3 (Kikuchi et al., 2003). Since the concentration of cefodizime in the extracellular fluid of the brain is less than the unbound plasma concentration (Matsushita et al., 1991), it could be that the efflux system for cefodizime is located in the blood-brain barrier. Further studies are necessary to investigate these transport mechanisms and the structure-activity relationships of cephalosporins governing their transport across the blood-brain barrier.

In conclusion, despite their very similar chemical structures, the elimination clearances of cefalexin and cefaclor from the CSF are markedly different. The results of the present study suggest that this distinction is accounted for by a difference in the contribution of the transporter responsible. A benzylpenicillin-sensitive transporter distinct from Oat3 accounts for the rapid elimination of cefaclor from the CSF, whereas a GlySar-sensitive transporter, presumably PEPT2, accounts for the elimination of cefalexin.

References

Cserr HF and Berman BJ (1978) Iodide and thiocyanate efflux from brain following injection into rat caudate nucleus. *Am J Physiol* **235**:F331–F337.

Dancer SJ (2001) The problem with cephalosporins. *J Antimicrob Chemother* **48**: 463–478.

Daniel H and Kottra G (2004) The proton oligopeptide cotransporter family SLC15 in physiology and pharmacology. *Pflugers Arch* **447**:610–618.

Ganapathy ME, Brandsch M, Prasad PD, Ganapathy V, and Leibach FH (1995) Differential recognition of β-lactam antibiotics by intestinal and renal peptide transporters, PEPT 1 and PEPT 2. *J Biol Chem* **270**:25672–25677.

Kikuchi R, Kusuhara H, Sugiyama D, and Sugiyama Y (2003) Contribution of organic anion transporter 3 (Slc22a8) to the elimination of p-aminohippuric acid and benzylpenicillin across the blood-brain barrier. *J Pharmacol Exp Ther* **306**: 51–58.

Kusuhara H, He Z, Nagata Y, Nozaki Y, Ito T, Masuda H, Meier PJ, Abe T, and Sugiyama Y (2003) Expression and functional involvement of organic anion transporting polypeptide subtype 3 (Slc21a7) in rat choroid plexus. *Pharm Res* **20**:720–727.

Kusuhara H, Sekine T, Utsunomiya-Tate N, Tsuda M, Kojima R, Cha SH, Sugiyama Y, Kanai Y, and Endou H (1999) Molecular cloning and characterization of a new multispecific organic anion transporter from rat brain. *J Biol Chem* **274**:13675–13680.

Levin VA (1980) Relationship of octanol/water partition coefficient and molecular weight to rat brain capillary permeability. *J Med Chem* **23**:682–684.

Lowry OH, Rosebrough NJ, Farr AL, and Randall RJ (1951) Protein measurement with folin phenol reagent. *J Biol Chem* **193**:265–267.

Matsushita H, Suzuki H, Sugiyama Y, Sawada Y, Iga T, Kawaguchi Y, and Hanano M (1991) Facilitated transport of cefodizime into the rat central nervous system. *J Pharmacol Exp Ther* **259**:620–625.

Nagata Y, Kusuhara H, Endou H, and Sugiyama Y (2002) Expression and functional characterization of rat organic anion transporter 3 (rOat3) in the choroid plexus. *Mol Pharmacol* **61**:982–988.

Nagata Y, Kusuhara H, Hirono S, Endou H, and Sugiyama Y (2004a) Carrier-mediated uptake of H2-receptor antagonists by the rat choroid plexus: involvement of rat organic anion transporter 3. *Drug Metab Dispos* **32**:1040–1047.

Nagata Y, Kusuhara H, Imaoka T, Endou H, and Sugiyama Y (2004b) Involvement of rat organic anion transporter 3 in the uptake of an organic herbicide, 2,4-dichlorophenoxyacetate, by the isolated rat choroid plexus. *J Pharm Sci* **93**:2724–2732.

Nohjoh T, Suzuki H, Sawada Y, Sugiyama Y, Iga T, and Hanano M (1989) Transport of cefodizime, a novel third generation cephalosporin antibiotic, in isolated rat choroid plexus. *J Pharmacol Exp Ther* **250**:324–328.

Novotny A, Xiang J, Stummer W, Teuscher NS, Smith DE, and Keep RF (2000) Mechanisms of 5-aminolevulinic acid uptake at the choroid plexus. *J Neurochem* **75**:321–328.

Ocheltree SM, Shen H, Hu Y, Xiang J, Keep RF, and Smith DE (2004) Mechanisms of cefadroxil uptake in the choroid plexus: studies in wild-type and PEPT2 knockout mice. *J Pharmacol Exp Ther* **308**:462–467.

Ogawa M, Suzuki H, Sawada Y, Hanano M, and Sugiyama Y (1994) Kinetics of active efflux via choroid plexus of beta-lactam antibiotics from the CSF into the circulation. *Am J Physiol* **266**:R392–R399.

Rothstein JD, Patel S, Regan MR, Haenggeli C, Huang YH, Bergles DE, Jin L, Dykes Hoberg M, Vidensky S, Chung DS, et al. (2005) Beta-lactam antibiotics offer neuroprotection by increasing glutamate transporter expression. *Nature (Lond)* **433**:73–77.

Smith DE, Johanson CE, and Keep RF (2004) Peptide and peptide analog transport systems at the blood-CSF barrier. *Adv Drug Deliv Rev* **56**:1765–1791.

Spector R (1987) Ceftriaxone transport through the blood-brain barrier. *J Infect Dis* **156**:209–211.

Spector R (1990) Advances in understanding the pharmacology of agents used to treat bacterial meningitis. *Pharmacology* **41**:113–118.

Sugiyama D, Kusuhara H, Shitara Y, Abe T, Meier PJ, Sekine T, Endou H, Suzuki H, and Sugiyama Y (2001) Characterization of the efflux transport of 17β-estradiol-D-17β-glucuronide from the brain across the blood-brain barrier. *J Pharmacol Exp Ther* **298**:316–322.

Suzuki H, Sawada Y, Sugiyama Y, Iga T, and Hanano M (1987) Transport of benzylpenicillin by the rat choroid plexus in vitro. *J Pharmacol Exp Ther* **242**: 660–665.

Suzuki H, Sawada Y, Sugiyama Y, Iga T, and Hanano M (1989a) Facilitated transport of benzylpenicillin through the blood-brain barrier in rats. *J Pharmacobiodyn* **12**:182–185.

Suzuki H, Sawada Y, Sugiyama Y, Iga T, Hanano M, and Spector R (1989b) Transport of imipenem, a novel carbapenem antibiotic, in the rat central nervous system. *J Pharmacol Exp Ther* **250**:979–984.

Suzuki H, Terasaki T, and Sugiyama Y (1997) Role of efflux transport across the blood-brain barrier and blood-cerebrospinal fluid barrier on the disposition of xenobiotics in the central nervous system. *Adv Drug Delivery Rev* **25**:257–285.

Tunkel AR and Scheld WM (1997) Issues in the management of bacterial meningitis. *Am Fam Physician* **56**:1355–1362.

Yamaoka K, Tanigawara Y, Nakagawa T, and Uno T (1981) A pharmacokinetic analysis program (multi) for microcomputer. *J Pharmacobiodyn* **4**:879–885.

Address correspondence to: Dr. Yuichi Sugiyama, 7-3-1 Hongo, Bunkyo-ku, Tokyo, Japan. E-mail: kusuhara@mol.f.u-tokyo.ac.jp

0022-3565/06/3162-647–653$20.00
THE JOURNAL OF PHARMACOLOGY AND EXPERIMENTAL THERAPEUTICS
Copyright © 2006 by The American Society for Pharmacology and Experimental Therapeutics
JPET 316:647–653, 2006

Vol. 316, No. 2
88328/3082565
Printed in U.S.A.

In Vivo Evaluation of P-glycoprotein Function at the Blood-Brain Barrier in Nonhuman Primates Using [^{11}C]Verapamil

Young-Joo Lee,[1] Jun Maeda, Hiroyuki Kusuhara, Takashi Okauchi, Motoki Inaji, Yuji Nagai, Shigeru Obayashi, Ryuji Nakao, Kazutoshi Suzuki, Yuichi Sugiyama, and Tetsuya Suhara

The Graduate School of Pharmaceutical Sciences, the University of Tokyo, Bunkyo-ku, Tokyo, Japan (Y.-J. L., H.K., Y.S.); Brain Imaging Project, National Institute of Radiological Sciences, Chiba, Japan (J.M., T.O., M.I., Y.N., S.O., T.S.); and Department of Medical Imaging, National Institute of Radiological Sciences, Chiba, Japan (R.N., K.S.)

Received April 21, 2005; accepted November 16, 2005

ABSTRACT

P-glycoprotein (P-gp) is a major efflux transporter contributing to the efflux of a range of xenobiotic compounds at the blood-brain barrier (BBB). In the present study, we evaluated the P-gp function at the BBB using positron emission tomography (PET) in nonhuman primates. Serial brain PET scans were obtained in three rhesus monkeys after intravenous administration of [^{11}C]verapamil under control and P-gp inhibition conditions ([PSC833 ([3′-keto-Me-Bmt^1]-[Val^2]-cyclosporin) 20 mg/kg/2 h]). The parent [^{11}C]verapamil and its metabolites in plasma were determined by HPLC with a positron detector. The initial brain uptake clearance calculated from the integration plot was used for the quantitative analysis. After intravenous administration, [^{11}C]verapamil was taken up rapidly into the brain (time to reach the peak, 0.58 min). The blood level of [^{11}C]verapamil decreased rapidly, and it underwent metabolism with time. The inhibition of P-gp by PSC833 increased the brain uptake of [^{11}C]verapamil 4.61-fold (0.141 versus 0.651 ml/g brain/min, $p < 0.05$). These results suggest that PET measurement with [^{11}C]verapamil can be used for the evaluation of P-gp function at the BBB in the living brain.

The blood-brain barrier (BBB), formed by brain-capillary endothelial cells, is a functional barrier responsible for restricting the entry of compounds from the circulating blood to the brain parenchyma cells (Reese and Karnovsky, 1967). The highly developed tight junctions between the adjacent brain cerebral endothelial cells are an anatomical feature of the BBB that minimizes the nonspecific penetration of compounds via paracellular route (Pardridge, 1988). In addition to this physical barrier, metabolic enzymes and active efflux transporters on this barrier also play important roles in BBB function. P-glycoprotein (P-gp), a 170-kDa membrane protein that is responsible for the multidrug resistance of tumor cells, is a major efflux transporter contributing to the efflux of a range of xenobiotic compounds in the circulating blood at the BBB (Schinkel et al., 1994; Tamai and Tsuji, 2000; Kusuhara and Sugiyama, 2001; Hirrlinger et al., 2002). Interestingly, P-gp may also be involved in the efflux of β-amyloid and has been suspected to play a role in Alzheimer's disease (Lam et al., 2001; Vogelgesang et al., 2002). In addition, a drug-drug interaction involving P-gp inhibition at the BBB has also been suggested (Sadeque at al., 2000). In a clinical study, when loperamide was administered with quinidine, a known P-gp inhibitor, respiratory depression by loperamide was induced (Sadeque at al., 2000). It is speculated that this is caused by modulation of the P-gp-mediated efflux by quinidine. Furthermore, a genetic polymorphism (C3435T) of P-gp has been reported to be associated with drug resistance in patients with epilepsy (Siddiqui et al., 2003), although a controversial result was reported recently (Tan et al., 2004). Such a genetic polymorphism may be associated with interindividual differences in drug concentration in the central nervous system.

This study was performed through the Advanced and Innovational Research program in Life Sciences from the Ministry of Education, Culture, Sports, Science and Technology, Japan. This work was also partially supported by a research grant from the Society of Japanese Pharmacopoeia and the Minister of Health, Labor and Welfare.

[1] Current affiliation: College of Pharmacy, Kyung Hee University, Seoul, Korea.

Article, publication date, and citation information can be found at http://jpet.aspetjournals.org.
doi:10.1124/jpet.105.088328.

ABBREVIATIONS: BBB, blood-brain barrier; ANOVA, analysis of variance; AUC, area under the curve; C_{max}, maximal concentration; HPLC, high-pressure liquid chromatography; MRI, magnetic resonance image; PET, positron emission tomography; P-gp, P-glycoprotein; PSC833, [3′-keto-Me-Bmt^1]-[Val^2]-cyclosporin; T_{max}, time to reach the C_{max}.

These clinical reports prompted a growing interest in the quantitative evaluation of P-gp function in living human brain.

Recently, in vivo evaluation of P-gp function was proposed using an imaging method with [^{11}C]colchicine, [^{11}C]carvedilol, [^{18}F]paclitaxel, and [^{11}C]verapamil (Elsinga et al., 2004). Hendrikse et al. (1998) demonstrated in rodents that the brain uptake of the P-gp substrate [^{11}C]verapamil was increased after pretreatment with cyclosporin A, a P-gp inhibitor, and they showed that that the distribution volume, estimated by Logan plot, was increased by pretreatment with cyclosporin A (Bart et al., 2003; Elsinga et al., 2004). As for human studies, Sasongko et al. (2005) demonstrated that the ratio of the area under the curve (AUC) of the brain concentration to that of blood concentration was increased in the presence of cyclosporin A, and Kortekaas et al. (2005) reported that the distribution volume of [^{11}C]verapamil in the midbrain was increased in Parkinson's disease patients compared with controls. In the present study, the P-gp function at the BBB was evaluated in rhesus monkeys by PET using [^{11}C]verapamil, with or without a potent P-gp inhibitor PSC833. PSC833 treatment caused a significant increase in the brain uptake clearance of [^{11}C]verapamil, which was determined using integration plot analysis using initial brain and blood concentration data.

Materials and Methods

Chemicals. The P-gp inhibitor PSC833 (Valspodar) was kindly supplied by Novartis (Basel, Switzerland) and was dissolved in Intralipid (Lo et al., 2001) (oil in water emulsion droplet; Otsuka Pharmaceutical, Tokyo, Japan). [^{11}C]Verapamil was synthesized from norverapamil (Eisai Co. Ltd., Tokyo, Japan) as described previously (Wegman et al., 2002) and diluted with approximately 2 to 3 ml 0.9% saline containing 0.75% polyoxyethylenemonosorbitan oleate and 1% ascorbic acid. The specific radioactivity of [^{11}C]verapamil used in all experiments ranged from 28.3 to 79.7 GBq/μmol (47.6 ± 17.3 GBq/μmol, mean ± S.D., radiochemical purity is over 95%).

Animals. Three young male rhesus monkeys (Macaca mulatta) weighing approximately 6.0 to 6.7 kg were used. The monkeys were maintained and handled in accordance with recommendations by the United States National Institutes of Health and our own guidelines (National Institute of Radiological Sciences, Chiba, Japan). The study was approved by the Animal Ethics Committee of the National Institute of Radiological Sciences. A magnetic resonance image (MRI) of each monkey brain was obtained beforehand.

PET Scan. All PET scans were performed using a high-resolution SHR-7700 PET camera (Hamamatsu Photonics, Shizuoka, Japan) designed for laboratory animals, which provides 31 transaxial slices 3.6 mm (center-to-center) apart, a 33.1-cm field of view, and spatial resolution of 2.6 mm full width at half-maximum (Watanabe et al., 1997). Monkeys were trained beforehand as being immobilized with the head fixation device to ensure accuracy of repositioning throughout the session (Obayashi et al., 2001). The infusion of PSC833 (20 mg/kg/2 h), a P-gp modulator, or vehicle alone to each monkey was started 1 h before the intravenous administration of [^{11}C]verapamil and maintained during the experiment. After administration of [^{11}C]verapamil, 0.9% saline was flushed into the catheter line to prevent adsorption or retention of verapamil. Arterial blood sampling (~0.5–1.5 ml) was performed via an indwelling arterial port from the saphenous artery at 10 s, 20 s, 30 s, 45 s, 1 min, 1.5 min, 3 min, 4.5 min, 6 min, 8 min, 10 min, 15 min, 20 min, 30 min, 45 min, and 60 min after administration, and the radioactivity in the blood was counted in a well-type γ-scintillation counter. Radioactivity was corrected for decay. After transmission scans for attenuation correction for 30 min, a dynamic emission scan in enhanced 2D mode was performed for 60 min (10 × 12 s, 30 × 6 s, 1 × 5 min, 2 × 5 min, and 5 × 8 min; a total of 36 frames). [^{11}C]Verapamil was administered via the saphenous vein as a single bolus at the start of the emission scan. The injected doses of [^{11}C]verapamil were 65.8 ± 11.5 MBq/kg (mean ± S.D.). The PET scans were separated by at least 4-week intervals and randomized for each monkey.

Metabolite Analysis. Arterial blood samples were collected at 1, 3, 6, 10, 15, 30, and 60 min after administration of [^{11}C]verapamil. Plasma was obtained by centrifugation and deproteinized with 2 volumes of acetonitrile. The supernatant was analyzed for radioactive components using a high-pressure liquid chromatography (HPLC) system (PU-610A series; GL Sciences, Torrance, CA) with a coupled NaI(Tl) positron detector (Takei et al., 2001) to measure [^{11}C]verapamil metabolites. Isocratic elution was performed with a reversed-phase semipreparative μ-Bondpak C18 column (7.8 × 300 mm i.d.; Waters, Milford, MA). The mobile phase consisted of a mixture of acetonitrile and 0.1 M ammonium acetate (70:30 v/v). The flow rate was 5 ml/min, and the injected sample size was 1.0 ml. The elute was monitored by ultraviolet absorbance at 254 nm and coupled NaI(Tl) positron detection. The percentage of parent radioactivity was determined from the activity of the parent verapamil with respect to the ^{11}C radioactivity in the chromatogram.

PET Data Analysis. All emission scan images were reconstructed with a 4.0-mm Hann filter, and regions of interest were placed on the whole cerebrum using PET Analyzer (in-house software, National Institute of Radiological Sciences; Maeda et al., 2001), and MRI information on each monkey. The summation images of [^{11}C]verapamil from 0 to 5 min were coregistered on the magnetic resonance images by means of statistical parametric mapping (SPM 2; Welcome Department of Cognitive Neurology, London, UK), and then the volume images were processed with Virtual Place TM (AZE Ltd. Tokyo, Japan). The decay-corrected ^{11}C radioactivity was normalized to the injected dose (% dose). The maximal ^{11}C radioactivity in the cerebrum (C_{max_cereb}) and the time to reach the C_{max_cereb} (T_{max_cereb}) were obtained from the time-^{11}C radioactivity data. The AUC was calculated for brain and blood, and it was calculated using data from 0 to 4.5 min after administration to minimize the bias by metabolites.

Integration Plot. The initial brain uptake was measured over a short period (~1–4.5 min) using integration plot method. The uptake rate of [^{11}C]verapamil can be described by the following equation,

$$\frac{X_{t,cereb}}{C_{t,blood}} = CL_{uptake} \times \frac{AUC_{(0-t)}}{C_{t,blood}} + V_E \qquad (1)$$

where CL_{uptake} is the brain uptake clearance based on the blood ^{11}C radioactivity, $X_{t,cereb}$ is the amount of ^{11}C radioactivity in the cerebrum at time t, and $C_{t,blood}$ is the blood concentration calculated from ^{11}C radioactivity. $AUC_{(0-t)}$ represents the area under the blood concentration curve from 0 to t, and V_E represents the initial distribution volume in the brain at time 0. V_E was obtained from the y-intercept of the integration plot and includes the distribution volume in blood residing within the brain as well as the initial distribution volume of [^{11}C]verapamil in the brain rapidly equilibrating with that in blood. Therefore, the CL_{uptake} value can be obtained from the initial slope of a plot of $X_{t,cereb}/C_{t,blood}$ versus $AUC_{(0-t)}/C_{t,blood}$, designated as the integration plot (Kim et al., 1988).

Inhibition of P-gp Function. The effect of PSC833, a P-gp modulator, was evaluated based on the normalized time-activity curves of brain and blood for the three monkeys, with and without PSC833 administration. PSC833 was infused at a dose of 20 mg/kg/2 h starting 1 h before intravenous administration of [^{11}C]verapamil and maintained until the end of the experiment (Song et al., 1999; Rodriguez et al., 2004). In a control experiment, drug vehicle was infused in the same manner. Differences were considered statistically significant when $p < 0.05$ using a one-sided paired t test, with the exception of the time course results in which two-way analysis of variance was used.

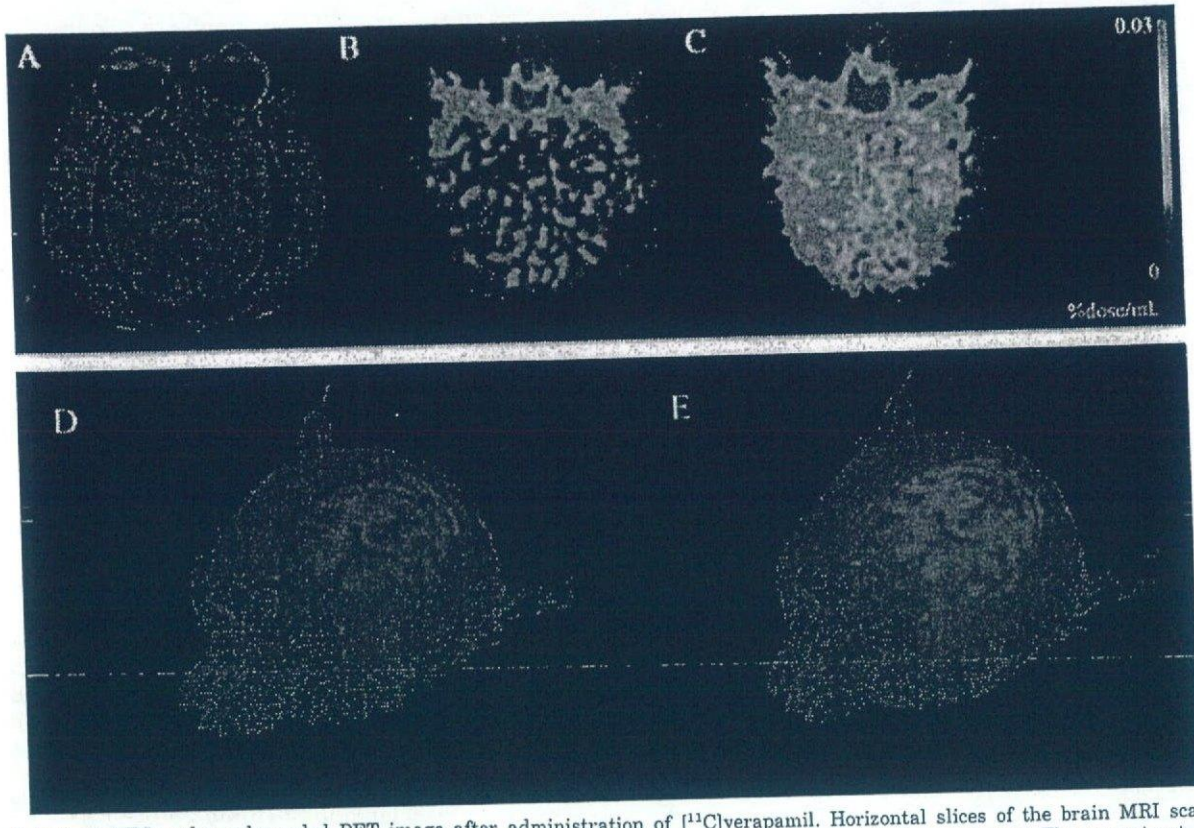

Fig. 1. A typical MRI and a color-coded PET image after administration of [^{11}C]verapamil. Horizontal slices of the brain MRI scans (A) and corresponding summation of PET images (B and C, up to 5 min) of the cerebral ^{11}C radioactivity uptake in one animal. The reconstructed MRI-PET image is also shown to assist intuitive understanding (D and E). B and D represent the control state, and C and E are the P-gp inhibition conditions obtained after PSC833 administration.

Results

The Distribution of [^{11}C]Verapamil in the Brain. A control PET image (Fig. 1B) accompanied by a corresponding morphological MRI (Fig. 1A) showed the uptake of ^{11}C radioactivity in the monkey brain. Higher uptake of ^{11}C radioactivity was observed in the brain after PSC833 treatment (Fig. 1C, PSC833-treated). Brain uptake was also clearly identified from PET/MRI-coregistered images (Fig. 1, D and E). The time-activity curves in the cerebrum are shown in Fig. 2. The ^{11}C radioactivity in the cerebrum peaked at 0.58 min after intravenous administration of [^{11}C]verapamil and remained almost constant at this level up to 60 min. Only limited amount of ^{11}C radioactivity (0.0105 ± 0.0006% dose/g brain, C_{max_cereb}, mean ± S.D.) was transported into the cerebrum.

Treatment with PSC833 significantly increased the ^{11}C radioactivity uptake in the cerebrum (two-way ANOVA, $p < 0.05$). The cerebrum AUC (AUC_{cereb}) of the PSC833 treatment group was significantly greater than that of the control group (1.96-fold) (Table 1; $p < 0.05$). The C_{max_cereb} of the PSC833 treatment group was also significantly higher than that of the control group (1.57-fold) (Table 1, $p < 0.05$). The T_{max_cereb} was not changed by treatment with PSC833 (Table 1).

Blood Profile and Metabolism of [^{11}C]Verapamil. The time-^{11}C radioactivity in the blood is shown in Fig. 3. The ^{11}C radioactivity in the blood fell quickly up to 3 min and then remained constant or slightly increased. Treatment with PSC833 did not affect the blood ^{11}C radioactivity profile (two-way ANOVA). The blood AUC (AUC_{blood}) of the PSC833 treatment group was similar to that of the control group (Table 1).

A chromatogram of the HPLC analysis of [^{11}C]verapamil, with or without treatment with PSC833, is shown in Fig. 4A. The retention time of verapamil was approximately 7 to 8 min. The fraction of intact verapamil decreased with time (Fig. 4B). At 10 min after administration, on average, approximately 25% of the radioactivity in plasma was the metabolite of [^{11}C]verapamil in the control group and intact verapamil represented approximately 50% of the radioactivity in the plasma of the control group 30 min after administration

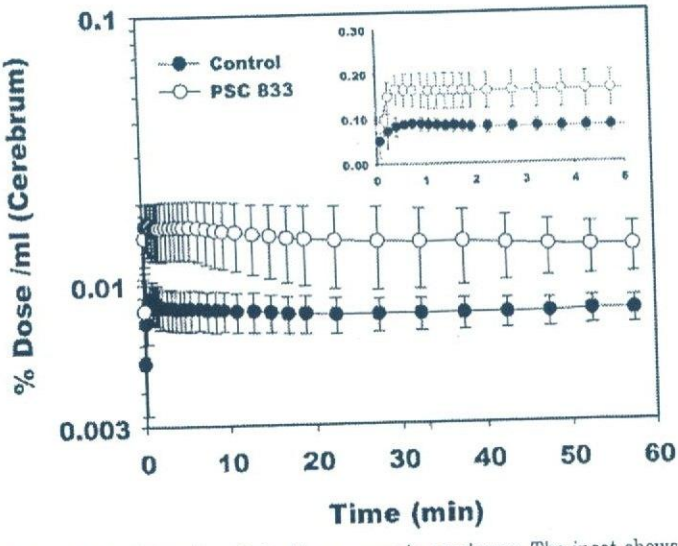

Fig. 2. The ^{11}C radioactivity time curves in cerebrum. The inset shows the detail curves in the early time period (mean ± S.D., $n = 3$). The treatment with PSC833 clearly increases the ^{11}C radioactivity in the cerebrum (two-way ANOVA, $p < 0.05$).

TABLE 1
Pharmacokinetic parameters of [^{11}C]verapamil after intravenous administration, with or without PSC833 (20 mg/kg/2 h)
The AUC_{blood} and AUC_{cereb} were calculated from 0 to 4.5 min after the administration using data shown in Figs. 2 and 3. CL_{uptake} and V_E were obtained from Figure 5. The values represent mean ± S.D. (n = 3). Data in parentheses indicate values from individual animals.

Pharmacokinetic Parameter	Control	+ PSC833 Treatment
AUC_{blood} (% dose × min/ml)	0.0567 ± 0.0145 (0.0461, 0.0733, 0.0507)	0.0535 ± 0.0331 (0.0418, 0.0279, 0.0909)
AUC_{cereb} (% dose × min/g)	0.0365 ± 0.0039 (0.0407, 0.0359, 0.0328)	0.0713 ± 0.0169* (0.0795, 0.0519, 0.0827)
C_{max_cereb} (% dose/g)	0.0105 ± 0.0006 (0.0104, 0.00989, 0.0112)	0.0166 ± 0.0033* (0.0185, 0.0128, 0.0192)
T_{max_cereb} (min)	0.58 ± 0.44 (1.08, 0.42, 0.25)	0.59 ± 0.29 (0.92, 0.42, 0.42)
CL_{uptake} (ml/g/min)	0.141 ± 0.043 (0.185, 0.139, 0.100)	0.651 ± 0.333* (0.937, 0.731, 0.285)
V_E (ml/g)	0.243 ± 0.130 (0.286, 0.0971, 0.346)	0.436 ± 0.279 (0.402, 0.731, 0.176)

* A statistically significant difference was observed (t test, $P < 0.05$).

(Fig. 4B). Treatment with PSC833 slightly increased the metabolite fraction in plasma (Fig. 4B; two-way ANOVA, $p < 0.05$). The inset in Fig. 3 shows the time-activity curves of intact [^{11}C]verapamil in plasma. The plasma radioactivity profile of intact [^{11}C]verapamil was not affected by treatment with PSC833 (two-way ANOVA).

The Brain Uptake Clearance of [^{11}C]Verapamil and Effect of PSC833. Integration plots of the control and PSC833 treatment studies of the three monkeys are shown in Fig. 5, A through C. The integration plots were linear over a short period, which varied from 1 min to 4.5 min, depending on the subject and with or without PSC833 treatment. During this period, the metabolite of [^{11}C]verapamil accounted for less than 12.5% ^{11}C radioactivity. The initial brain uptake of the control group was 0.141 ml/g/min (0.141 ± 0.043, mean ± S.D.), and this was increased after PSC833 treatment (0.651 ± 0.333 ml/g brain/min, mean ± S.D., $p < 0.05$). The V_E was not changed by PSC833 treatment (Table 1). The AUC_{cereb}/AUC_{blood} ratio of ^{11}C radioactivity was increased 2.31-fold in the presence of PSC833.

Discussion

In this study, we evaluated the P-gp function at the BBB in vivo using PET with [^{11}C]verapamil. Recently, the use of imaging techniques, such as single photon emission-computed tomography and PET using [^{11}C]colchicine, [^{11}C]carvedilol, [^{18}F]paclitaxel, and [^{64}Cu]complexes and [^{68}Ga]complexes and [^{99m}Tc]complexes, has been suggested for the noninvasive evaluation of P-gp function in vivo (Elsinga et al., 2004). Among these compounds, [^{11}C]verapamil is a well characterized PET ligand for evaluating P-gp function at the BBB (Hendrikse et al., 1998, 1999), and verapamil can be easily labeled with ^{11}C using commercially available norverapamil (Wegman et al., 2002).

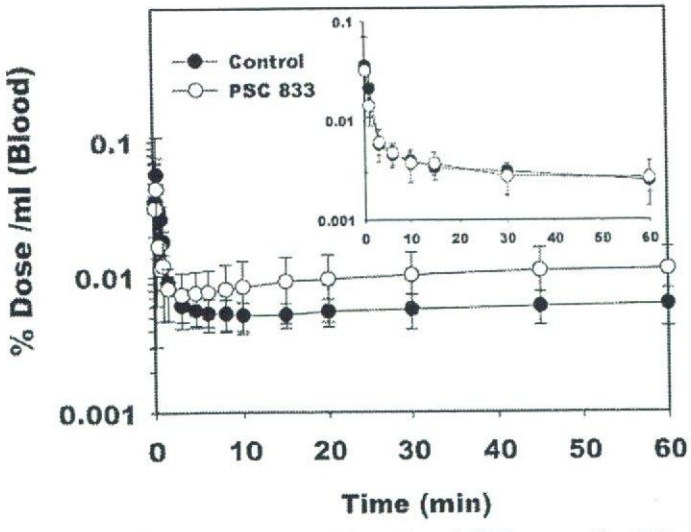

Fig. 3. The [^{11}C]radioactivity and intact (inset) [^{11}C]verapamil activity-time curves in cerebrum and blood. The time-^{11}C radioactivity and intact [^{11}C]verapamil activity curves in blood are similar for both the control and PSC833 treatment groups (mean ± S.D., n = 3).

After intravenous administration of [^{11}C]verapamil, it was rapidly distributed in the brain over a short period and then was eliminated slowly (Fig. 2). Apparently, the ^{11}C radioactivity reached a distributional pseudoequilibrium within a short period (Fig. 3). This is similar to earlier results obtained in rats (Hendrikse et al., 1999). The uptake of ^{11}C radioactivity into the cerebrum increased after PSC833 treatment (Figs. 1 and 2). PSC833 treatment increased the AUC_{cereb} and C_{max_cereb} of ^{11}C radioactivity compared with the values obtained in the control group (Table 1). These data indicate that the efflux transport by P-gp affects the initial brain uptake and that the inhibition of P-gp-mediated transport increases the brain uptake of P-gp substrates (Kusuhara et al., 1997; Dagenais et al., 2000) and supports recent human brain PET study using [^{11}C]verapamil, which was published during the revision process of this manuscript (Sasongko et al., 2005).

The blood concentration-time profile of the ^{11}C radioactivity was biphasic, exhibiting a rapid reduction within minutes followed by an increase in the ^{11}C radioactivity (Fig. 3). The increase at later time points was more marked in the PSC833-treated group than in the control group. The ^{11}C radioactivity in the blood specimens includes unchanged [^{11}C]verapamil and its metabolites (Fig. 4A). Approximately 75% of the ^{11}C radioactivity was unchanged [^{11}C]verapamil during the initial 10 min, and the fraction of the unchanged form in the blood specimens rapidly decreased (Fig. 4B). This observation is consistent with the previous reports of verapamil metabolism in humans (Kroemer et al., 1993; von Richter et al., 2000; von Richter et al., 2001) and monkeys (Link, 2003), whereas low levels of the metabolite of [^{11}C]verapamil during PET studies have been reported in rodents (Hendrikse et al., 1998, 1999). Because the increase at later time points was not observed in the blood concentration-time profile of unchanged [^{11}C]verapamil (Fig. 3, inset), it is likely that the increase is due to the accumulation of metabo-

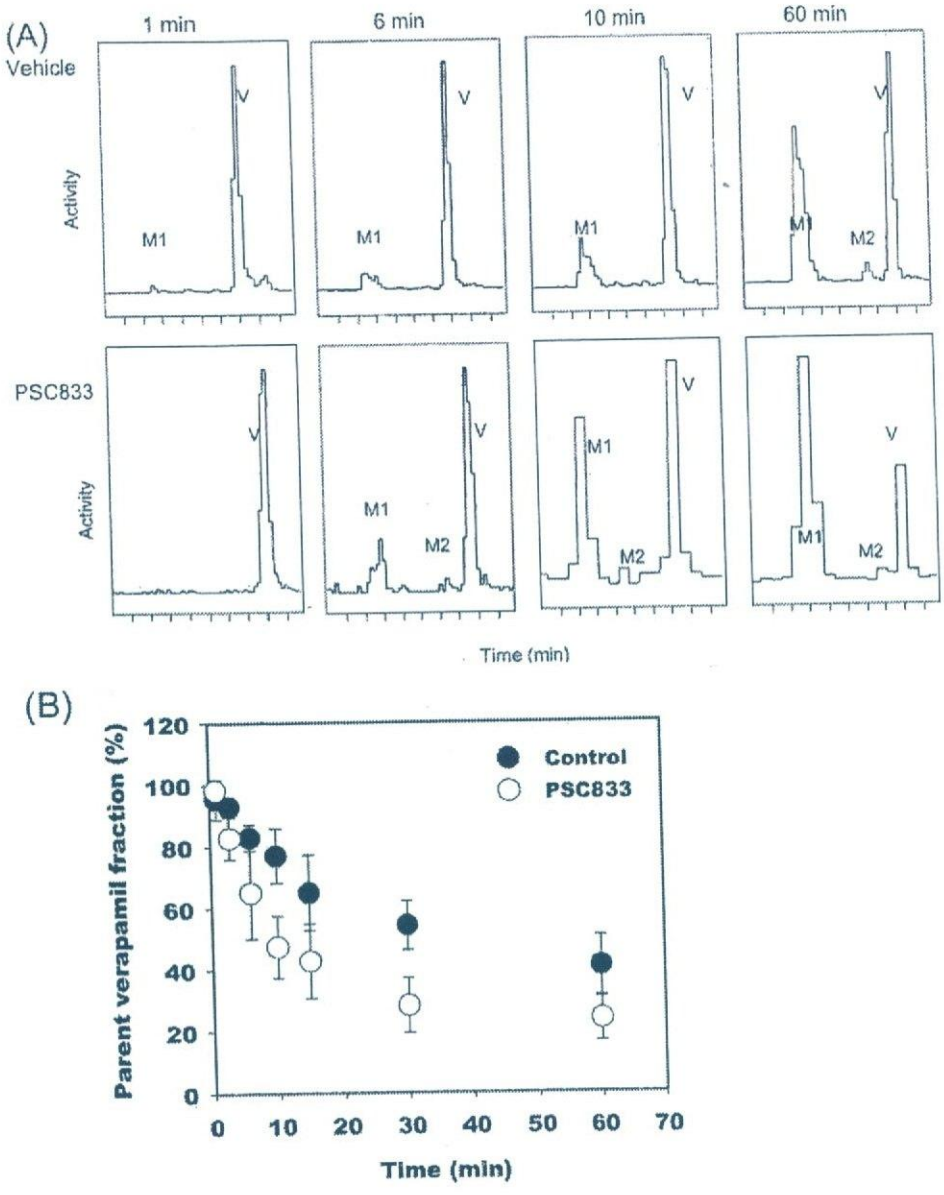

Fig. 4. A, typical chromatograms of plasma samples at 1, 6, 10, and 60 min after intravenous administration of [^{11}C]verapamil, with or without PSC833. B, parent [^{11}C]verapamil fraction of the ^{11}C radioactivity in plasma. The parent verapamil was detected at approximately 7 to 8 min (V). HPLC analysis suggested that there are at least two metabolites (M1, M2) of verapamil after intravenous administration. The parent fraction of verapamil in plasma fell rapidly with time. At 10 min after administration, on average, approximately 75% of the radioactivity in plasma was due to the parent verapamil in the control group and the parent verapamil represented approximately 50% of the radioactivity in the plasma of the control group 30 min after administration (mean ± S.D., n = 3).

lites in the blood from the peripheral tissues. Since PSC833 is known to be a fairly specific P-gp inhibitor with a low degree of metabolic inhibition (Kawahara et al., 2000) and metabolites of verapamil are also substrates of P-gp with a range of specificities (Pauli-Magnus et al., 2000), PSC833 treatment may cause a delay in the elimination of metabolized verapamil, resulting in marked plasma accumulation of metabolites.

Because we could not separate metabolites from parent verapamil in brain, there is a possibility that different parent/metabolite ratio might exist in the brain compared with blood. To deal with this extensive metabolism of [^{11}C]verapamil, we used the initial PET data (~0–4.5min) to avoid any bias from metabolites. Integration plot analysis has been used to obtain a tissue-specific uptake clearance. The initial PET scan data (from 0 to ~1–4.5 min, depending on the subjects) was enough to calculate the initial uptake clearance, during which no extensive metabolism of verapamil was observed (Fig. 4). Figure 5 shows the integration plot of the blood versus tissue time-activity curves in three monkeys (Fig. 5). The CL_{uptake} calculated from the slope of the integration plot increased after treatment with PSC833. This indicates the modulation of P-gp function at the BBB by PSC833 (Table 1) (Kusuhara et al., 1997; Song et al., 1999). The initial brain uptake clearance of [^{11}C]verapamil is a sensitive parameter for P-gp function at the BBB. However, the magnitude of the increase observed in PSC833-treated monkeys was not as high as that observed in P-gp knockout mice. This may be explained by incomplete inhibition of P-gp activity by PSC833, variable brain concentration of PSC833 in monkey, and, partly, a species difference in P-gp expression and/or intrinsic efflux transport activity. In fact, PSC833 treatment does not fully inhibit P-gp function at the BBB in mice (Kusuhara et al., 1997). Interestingly, recent human [^{11}C]verapamil PET study in the presence of cyclosporin A showed a similar degree of increase in the brain distribution of verapamil by P-gp inhibition. In this study, the AUC_{cereb}/AUC_{blood} ratio of ^{11}C radioactivity was increased 1.88-fold in the presence of cyclosporin A, which was consistent with the present study (2.31-fold) (Sasongko et al., 2005). This supports the belief that the species difference in the role of P-gp

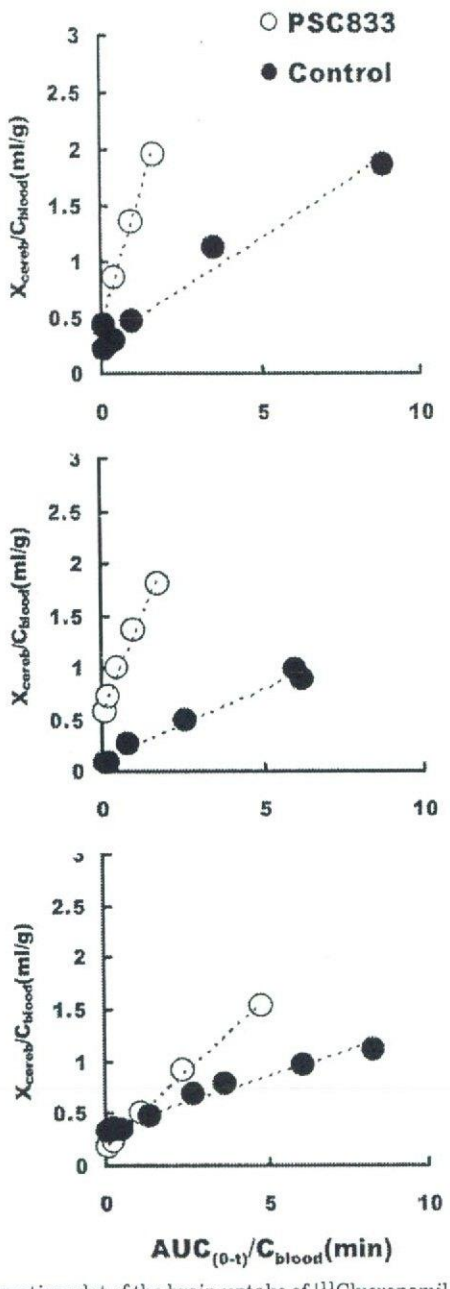

Fig. 5. Integration plot of the brain uptake of [^{11}C]verapamil for the three monkeys (A, B, and C). The initial brain uptake of the control group was increased after treatment with PSC833 (t test, $p < 0.05$, $n = 3$). The V_E was not changed by PSC833 treatment.

at the BBB may not be very significant between humans and monkeys and suggests the feasibility of a PET study using monkeys to provide information on the human BBB. Unlike the slope, the y-intercept of the plot was insensitive to the PSC833 treatment (Table 1). The y-intercept represents the initial distribution volume, including the vascular space and rapid adsorption/binding to the vascular surface, which can achieve rapid equilibrium with the blood compartment. Because the initial distribution volume is greater than the vascular space in the brain, estimated to be 35μl/g brain in 15 adult rhesus monkeys (Eichling et al., 1975), it seems that the adsorption/binding of [^{11}C]verapamil to the vascular surface occurs within a short period. The use of integration plot analysis helps in the quantitative investigation of P-gp function at the BBB without any interference from the rapid and extensive metabolism of [^{11}C]verapamil, which makes it inappropriate to use common graphical methods that need data obtained from long-term sampling (Logan, 2003).

In conclusion, we have been able to evaluate P-gp function at the BBB in nonhuman primates, using [^{11}C]verapamil as a PET ligand and integration plot method. P-gp at the BBB has attracted much interest from a clinical point of view; i.e., drug-drug interactions and the effects of genetic polymorphisms. Therefore, in future, PET studies using [^{11}C]verapamil will be a powerful tool for evaluating P-gp function at the BBB in a noninvasive manner.

Acknowledgments

We thank the members of the Cyclotron Unit and Radiopharmaceutical and Radiopharmacological Section for operation of the cyclotron and the production of radioisotopes, Novartis Pharm AG for its kind gift of PSC833, and Eisai Co. Ltd. for its kind gift of norverapamil.

References

Bart J, Willemsen AT, Groen HJ, van der Graaf WT, Wegman TD, Vaalburg W, de Vries EG, and Hendrikse NH (2003) Quantitative assessment of P-glycoprotein function in the rat blood-brain barrier by distribution volume of [^{11}C]verapamil measured with PET. *Neuroimage* **20**:1775–1782.

Dagenais C, Rousselle C, Pollack GM, and Scherrmann JM (2000) Development of an in situ mouse brain perfusion model and its application to mdr1a P-glycoprotein-deficient mice. *J Cereb Blood Flow Metab* **20**:381–386.

Eichling JO, Raichle ME, Grubb RL Jr, Larson KB, and Ter-Pogossian MM (1975). In vivo determination of cerebral blood volume with radioactive oxygen-15 in the monkey. *Circ Res* **37**:707–714.

Elsinga PH, Hendrikse NH, Bart J, Vaalburg W, and van Waarde A (2004) PET studies on P-glycoprotein function in the blood-brain barrier: how it affects uptake and binding of drugs within the CNS. *Curr Pharm Des* **10**:1493–1503.

Hendrikse N, Schinkel A, de Vries E, Fluks E, Van der Graaf W, Willemsen A, Vaalburg W, and Franssen E (1998) Complete in vivo reversal of P-glycoprotein pump function in the blood- brain barrier visualized with positron emission tomography. *Br J Pharmacol* **124**:1413–1418.

Hendrikse NH, de Vries EG, Eriks-Fluks L, van der Graaf WT, Hospers GA, Willemsen AT, Vaalburg W, and Franssen EJ (1999) A new in vivo method to study P-glycoprotein transport in tumors and the blood-brain barrier. *Cancer Res* **59**: 2411–2416.

Hirrlinger J, Konig J, and Dringen R (2002) Expression of mRNAs of multidrug resistance proteins (Mrps) in cultured rat astrocytes, oligodendrocytes, microglial cells and neurones. *J Neurochem* **82**:716–719.

Kawahara I, Kato Y, Suzuki H, Achira M, Ito K, Crespi CL, and Sugiyama Y (2000) Selective inhibition of human cytochrome P450 3A4 by *N*-[2(*R*)-hydroxy-1(*S*)-indanyl]-5-[2(*S*)-(1,1-dimethylethylaminocarbonyl)-4-[(furo[2, 3-b]pyridin-5-yl)methyl]piperazin-1-yl]-4(*S*)-hydroxy-2(*R*)-phenylmethylpentanamide and P-glycoprotein by valspodar in gene transfectant systems. *Drug Metab Dispos* **28**: 1238–1243.

Kim DC, Sugiyama Y, Satoh H, Fuwa T, Iga T, and Hanano M (1988) Kinetic analysis of in vivo receptor-dependent binding of human epidermal growth factor by rat tissues. *J Pharm Sci* **77**:200–207.

Kortekaas R, Leenders KL, van Oostrom JC, Vaalburg W, Bart J, Willemsen AT, and Hendrikse NH (2005) Blood-brain barrier dysfunction in parkinsonian midbrain in vivo. *Ann Neurol* **57**:176–179.

Kroemer HK, Gautier JC, Beaune P, Henderson C, Wolf CR, and Eichelbaum M (1993) Identification of P450 enzymes involved in metabolism of verapamil in humans. *Naunyn-Schmiedeberg's Arch Pharmacol* **348**:332–337.

Kusuhara H and Sugiyama Y (2001) Efflux transport systems for drugs at the blood-brain barrier and blood-cerebrospinal fluid barrier (part 1). *Drug Discov Today* **6**:150–156.

Kusuhara H, Suzuki H, Terasaki T, Kakee A, Lemaire M, and Sugiyama Y (1997) P-glycoprotein mediates the efflux of quinidine across the blood-brain barrier. *J Pharmacol Exp Ther* **283**:574–580.

Lam FC, Liu R, Lu P, Shapiro AB, Renoir JM, Sharom FJ, and Reiner PB (2001) β-Amyloid efflux mediated by p-glycoprotein. *J Neurochem* **76**:1121–1128.

Link JM (2003) PET imaging of in vivo transporter and receptor activity, in *AAPS Workshop on Drug Transport: From the Bench to the Bedside*, Wyndham Peachtree Conference Center, Peachtree City, GA.

Logan J (2003) A review of graphical methods for tracer studies and strategies to reduce bias. *Nucl Med Biol* **30**:833–844.

Lo Y, Liu F, and Cherng J (2001) Effect of PSC 833 liposomes and Intralipid on the transport of epirubicin in Caco-2 cells and rat intestines. *J Control Release* **76**:1–10.

Maeda J, Suhara T, Ogawa M, Okauchi T, Kawabe K, Zhang MR, Semba J, and Suzuki K (2001) In vivo binding properties of [carbonyl-^{11}C]WAY-100635: effect of endogenous serotonin. *Synapse* **40**:122–129.

Obayashi S, Suhara T, Kawabe K, Okauchi T, Maeda J, Akine Y, Onoe H, and Iriki A (2001) Functional brain mapping of monkey tool use. *Neuroimage* **14**:853–861.

Pardridge WM (1988) Recent advances in blood-brain barrier transport. *Annu Rev Pharmacol Toxicol* **28**:25–39.
Pauli-Magnus C, von Richter O, Burk O, Ziegler A, Mettang T, Eichelbaum M, and Fromm MF (2000) Characterization of the major metabolites of verapamil as substrates and inhibitors of P-glycoprotein. *J Pharmacol Exp Ther* **293**:376–382.
Reese TS and Karnovsky MJ (1967) Fine structural localization of a blood-brain barrier to exogenous peroxidase. *J Cell Biol* **34**:207–217.
Rodriguez M, Ortega I, Soengas I, Suarez E, Lukas JC, and Calvo R (2004) Effect of P-glycoprotein inhibition on methadone analgesia and brain distribution in the rat. *J Pharm Pharmacol* **56**:367–374.
Sadeque AJ, Wandel C, He H, Shah S, and Wood AJ (2000) Increased drug delivery to the brain by P-glycoprotein inhibition. *Clin Pharmacol Ther* **68**:231–237.
Sasongko L, Link JM, Muzi M, Mankoff DA, Yang X, Collier AC, Shoner SC, and Unadkat JD (2005) Imaging P-glycoprotein transport activity at the human blood-brain barrier with positron emission tomography. *Clin Pharmacol Ther* **77**:503–514.
Schinkel AH, Smit JJ, van Tellingen O, Beijnen JH, Wagenaar E, van Deemter L, Mol CA, van der Valk MA, Robanus-Maandag EC, te Riele HP, et al. (1994) Disruption of the mouse mdr1a P-glycoprotein gene leads to a deficiency in the blood-brain barrier and to increased sensitivity to drugs. *Cell* **77**:491–502.
Siddiqui A, Kerb R, Weale ME, Brinkmann U, Smith A, Goldstein DB, Wood NW, and Sisodiya SM (2003) Association of multidrug resistance in epilepsy with a polymorphism in the drug-transporter gene ABCB1. *N Engl J Med* **348**:1442–1448.
Song S, Suzuki H, Kawai R, and Sugiyama Y (1999) Effect of PSC 833, a P-glycoprotein modulator, on the disposition of Vincristine and digoxin in rats. *Drug Metab Dispos* **27**:689–694.
Takei M, Kida T, and Suzuki K (2001) Sensitive measurement of positron emitters eluted from HPLC. *Appl Radiat Isot* **55**:229–234.
Tamai I and Tsuji A (2000) Transporter-mediated permeation of drugs across the blood-brain barrier. *J Pharm Sci* **89**:1371–1388.
Tan NC, Heron SE, Scheffer IE, Pelekanos JT, McMahon JM, Vears DF, Mulley JC, and Berkovic SF (2004) Failure to confirm association of a polymorphism in ABCB1 with multidrug-resistant epilepsy. *Neurology* **63**:1090–1092.
Vogelgesang S, Cascorbi I, Schroeder E, Pahnke J, Kroemer HK, Siegmund W, Kunert-Keil C, Walker LC, and Warzok RW (2002) Deposition of Alzheimer's β-amyloid is inversely correlated with P-glycoprotein expression in the brains of elderly non-demented humans. *Pharmacogenetics* **12**:535–541.
von Richter O, Eichelbaum M, Schonberger F, and Hofmann U (2000) Rapid and highly sensitive method for the determination of verapamil, [2H7]verapamil and metabolites in biological fluids by liquid chromatography-mass spectrometry. *J Chromatogr B Biomed Sci Appl* **738**:137–147.
von Richter O, Greiner B, Fromm MF, Fraser R, Omari T, Barclay ML, Dent J, Somogyi AA, and Eichelbaum M (2001) Determination of in vivo absorption, metabolism and transport of drugs by the human intestinal wall and liver with a novel perfusion technique. *Clin Pharmacol Ther* **70**:217–227.
Watanabe M, Okada H, Shimizu K, Omura T, Yoshikawa E, Kosugi T, Mori S, and Yamashita T (1997) A high resolution animal PET scanner using compact PS-PMT detectors. *IEEE Trans Nucl Sci* **44**:1277–1282.
Wegman TD, Maas B, Elsinga PH, and Vaalburg W (2002) An improved method for the preparation of [^{11}C]verapamil. *Appl Radiat Isot* **57**:505–507.

Address correspondence to: Dr. Tetsuya Suhara, Brain Imaging Project, National Institute of Radiological Sciences, 9-1, Anagawa 4-Chome, Inage-ku, Chiba 263-8555, Japan. E-mail: suhara@nirs.go.jp

Quantitative Analysis of ^{11}C-Verapamil Transfer at the Human Blood–Brain Barrier for Evaluation of P-glycoprotein Function

Yoko Ikoma[1], Akihiro Takano[1], Hiroshi Ito[1], Hiroyuki Kusuhara[2], Yuichi Sugiyama[2], Ryosuke Arakawa[1,3], Toshimitsu Fukumura[4], Ryuji Nakao[4], Kazutoshi Suzuki[4], and Tetsuya Suhara[1]

[1]Department of Molecular Neuroimaging, Molecular Imaging Center, National Institute of Radiological Sciences, Chiba, Japan; [2]Department of Molecular Pharmacokinetics, Graduate School of Pharmaceutical Sciences, University of Tokyo, Tokyo, Japan; [3]Department of Neuropsychiatry, Nippon Medical School, Tokyo, Japan; and [4]Department of Radiochemistry, Molecular Imaging Center, National Institute of Radiological Sciences, Chiba, Japan

P-glycoprotein in the blood–brain barrier (BBB) has been found to be associated with several types of neurologic damage. ^{11}C-Verapamil has been used for in vivo imaging of P-glycoprotein function in the BBB by PET, but metabolites in plasma complicate the quantitative analysis of human studies. In this study, we validated the quantification methods of ^{11}C-verapamil transfer from plasma to the brain in humans. **Methods:** The transfer rate constant from plasma to the brain, K_1, was estimated by nonlinear least squares (NLS) with a 2-input compartment model, including the permeation of the main metabolite in plasma at the BBB, and with a 1-input compartment model using only 15-min data that contained little metabolite in plasma. K_1 was also estimated by graphical analysis of an integration plot that uses only early-time data, before the appearance of metabolites, and the estimated K_1 was compared with that obtained by the NLS method. In the simulation study, the reliability of parameter estimates in the graphical analysis method was investigated for various values of rate constants, time ranges of parameter estimations, and noise levels. **Results:** ^{11}C-Verapamil in plasma gradually converted to its metabolites, and about 45% of the radioactivity in the plasma specimen was associated with ^{11}C-verapamil metabolites at 30 min after injection. Although K_1 estimated from graphical analysis was slightly smaller than that by NLS, there was strong correlation among the K_1 values obtained by these 3 methods. In the simulation study, for graphical analysis, the differences between the true and mean of K_1 estimates became larger and the coefficient of variation (COV) of K_1 estimates became smaller as the end time of linear regression became later. The COV of graphical analysis was almost equal to that of NLS with the 1-input compartment model. **Conclusion:** The transfer of ^{11}C-verapamil from plasma to the brain was able to be quantitatively estimated by graphical analysis because this method can provide K_1 from the data of the initial few minutes without considering the effect of the metabolites in plasma.

Received Feb. 8, 2006; revision accepted May 10, 2006.

For correspondence or reprints contact: Hiroshi Ito, MD, PhD, Department of Molecular Neuroimaging, Molecular Imaging Center, National Institute of Radiological Sciences, 4-9-1, Anagawa, Inage-ku, Chiba, 263-8555, Japan.
E-mail: hito@nirs.go.jp

Key Words: ^{11}C-verapamil; PET; P-glycoprotein; blood–brain barrier; transfer rate constant

J Nucl Med 2006; 47:1531–1537

P-glycoprotein (P-gp) is found at cell membranes of various organs, and functions as an efflux pump hampering the invasion of toxic compounds into the cells (*1–4*). P-gp is also expressed at the blood–brain barrier (BBB), a functional barrier between blood and brain interstitial space formed by a continuous endothelial lining of cerebral capillaries, and plays indispensable roles as one of the barrier functions in BBB (*5–8*). In addition to its pharmacologic importance, P-gp in BBB was recently found to be associated with several neurologic disorders (*9,10*).

^{11}C-Verapamil has been used for in vivo neuroimaging of the brain by PET, representing a potent tool for imaging the function of P-gp (*11–14*). Some investigators analyzed the kinetics of ^{11}C-verapamil by the distribution volume (DV) estimated from the graphical analysis developed by Logan et al. (*15*) in rodents, reporting that the DV was increased by the pretreatment of cyclosporin A (CsA), a P-gp inhibitor (*16,17*). In a human study, Sasongko et al. demonstrated that the ratio of the area under the curve of brain to that of blood was increased in the presence of CsA (*18*), and Kortekaas et al. reported that the uptake of ^{11}C-verapamil as evaluated by the DV with the graphical analysis of Logan et al. was elevated in the midbrain of Parkinson's disease patients as compared with control subjects (*19*). On the other hand, Lee et al. evaluated the transfer of ^{11}C-verapamil from blood to brain with the graphical analysis using early-time data, the so-called integration plot, in rhesus monkeys with or without treatment of a P-gp inhibitor, PSC833, demonstrating that the brain uptake of ^{11}C-verapamil was increased after the PSC833 treatment (*20*). Moreover, Muzi et al. estimated the rate constant of ^{11}C-verapamil transfer to the brain, K_1, with 1- and 2-tissue compartment models in healthy

volunteers, reporting that K_1 increased in the presence of the P-gp inhibitor CsA (*21*). This means that the initial brain uptake of ^{11}C-verapamil can be an indicator of the P-gp activity at the BBB. However, Sasongko et al. reported that the plasma radioactivity of verapamil was approximately 35%, that of the main metabolite D-617 was 20% at 45 min, and that D-617 and several other minor metabolites might contribute to the image (*18*). Although these metabolites in plasma complicate the quantitative analysis, validation of these kinetic analysis methods for ^{11}C-verapamil has not been sufficiently confirmed in humans.

In this study, we evaluated the quantitative analysis methods to estimate the transfer of ^{11}C-verapamil from plasma to the brain in healthy volunteers, and the reliability of the estimated parameters was investigated by computer simulation.

MATERIALS AND METHODS

Subjects

Ten subjects (age range, 20–31 y; mean age ± SD, 23.8 ± 3.3 y) participated in this study. All volunteers were free of any somatic, neurologic, or psychiatric disorders, and they had no history of current or previous drug abuse. This study was approved by the Ethics and Radiation Safety Committees of the National Institute of Radiological Sciences, Chiba, Japan, and written informed consent was obtained from each subject.

Radioligand

^{11}C-Verapamil was synthesized from norverapamil (Eisai Co. Ltd.) as described previously (*22*).

PET

PET scans were performed using an ECAT EXACT 47 scanner (CTI/Siemens), which provides 47 planes and a 16.2-cm axial field of view. A transmission scan with a 3-rod source of ^{68}Ge-^{68}Ga was followed by a dynamic 60-min scan (15 s × 8, 30 s × 4, 60 s × 2, 120 s × 1, 240 s × 4, 360 s × 6) with a bolus injection of 629.0–856.9 MBq (mean ± SD, 746.3 ± 58.2 MBq) of ^{11}C-verapamil. The specific radioactivities were 31.0–99.3 GBq/μmol (mean ± SD, 48.1 ± 20.6 GBq/μmol) at the time of injection. The PET data were acquired in 2-dimensional mode and the data were reconstructed by filtered backprojection using a ramp filter with a cutoff frequency of 0.5.

MRI was performed with a Gyroscan NT scanner (1.5 T) (Phillips Medical Systems) to obtain T1-weighted images of the brain.

The PET images were coregistered to MR images, and regions of interest (ROIs) were defined over the frontal, temporal, parietal, and occipital cortices, and the cerebellum with a template-based method as described by Yasuno et al. (*23*).

Arterial Blood Sampling

To obtain the arterial input function, an automated blood sampling system was used during the first 5 min of each PET measurement (*24*). The concentration of radioactivity in arterial blood was measured every second. At the same time, arterial blood samples were taken manually and their radioactive concentrations were measured 26 times during the scan. Each manually taken blood sample was centrifuged to obtain plasma and blood cell fractions, and the concentration of radioactivity in the plasma was measured. Radioactivity between PET and blood was calibrated with a cylinder phantom and ^{18}F solution. Plasma metabolites were analyzed as follows: For the plasma fractions at 2, 4, 7, 12, 19, 29, 42, and 59 min after injection, acetonitrile was added and then centrifuged. The supernatant was analyzed for radioactive components using a high-performance liquid chromatography system (PU-610A series; GL Sciences) with a coupled bismuth germanate positron detector (*25*) to measure plasma ^{11}C-verapamil metabolites. Isocratic elution was performed with a reversed-phase semipreparative Waters μBondpak C_{18} column (7.8 mm [inner diameter] × 300 mm). The mobile phase consisted of a mixture of acetonitrile and 0.1 mol/L ammonium acetate (70:30, v/v). The percentage of parent radioactivity was determined from the activity of the parent verapamil with respect to the total activity in the chromatogram.

Data Analysis

2-Input Compartment Model. The rate constants between plasma and tissue were estimated both for unmetabolized ^{11}C-verapamil and for the main metabolite with a 2-input, 2-tissue compartment model including transfer of the metabolite from plasma to brain (Fig. 1) (*26,27*). K_1 describes the rate constant for transfer of ^{11}C-verapamil from plasma to brain, k_2 describes the rate constant for transfer of ^{11}C-verapamil from brain to plasma, and K_1^M and k_2^M represent the transfer of the main metabolite between plasma and brain. The fraction of unchanged ^{11}C-verapamil in the total plasma radioactivity was fitted by a 2-exponential expression (*28*), $f = a \times \exp(-bt) + (1 - a) \times \exp(-ct)$, where f is the fraction of unchanged ^{11}C-verapamil, and a, b, and c are the estimated parameters. A plasma curve of unchanged ^{11}C-verapamil used as input function C_p was generated by the product of the plasma activity and the fraction curves of unchanged ^{11}C-verapamil. Meanwhile, the fraction of the main metabolite in total plasma radioactivity was fitted by $f' = 1 - \{a' \times \exp(-b't) + (1 - a') \times \exp(-c't)\}$, where f′ is the fraction of the main metabolite, and a′, b′, and c′ are the estimated parameters. A plasma curve of the

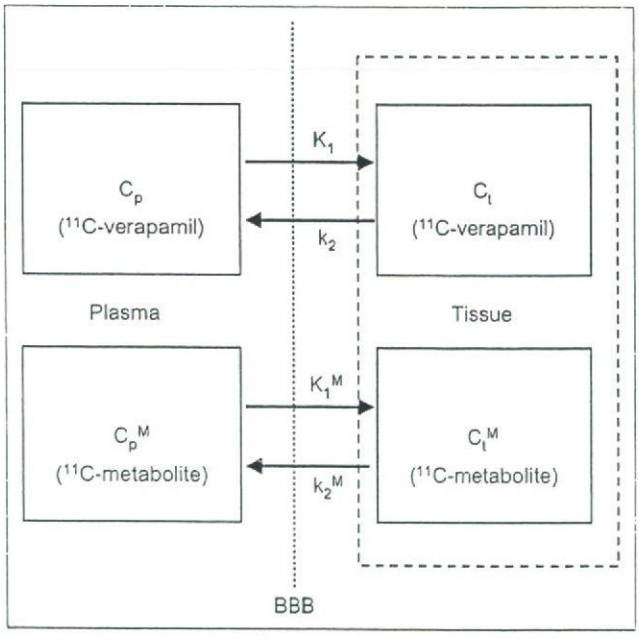

FIGURE 1. The 2-input, 2-tissue compartment model including transfer of metabolite in plasma to tissue.